and 0.002% (w/v) DNase I (Sigma–Aldrich) for 40 min at 37°C. Cells were overlaid on Lymphocyte M (Cedarlane Laboratories, Canada) in PBS.[27]

Fluorescence-activated cell sorter (FACS) analysis

The cells were surface-stained with FITC-conjugated anti-CD3 and APC-conjugated anti-NK1.1 mAbs, along with anti-interferon gamma (IFN-γ)-PE and anti-tumor necrosis factor alpha (TNF-α)-PE mAbs for intracellular cytokine detection (BD PharMingen). Samples were acquired using a FACSCalibur flow cytometer, and the data were analyzed using the CELLQuest software (BD Immunocytometry Systems, CA, USA). Apoptosis of IHLs was determined using annexin V-FITC and Via-Probe (a 7-amino-actinomycin D (7-AAD) viability probe) (PharMingen), according to the manufacturer's instructions.

BrdU incorporation

For *in vivo* BrdU labeling, mice received a 100-μL i.p. injection of a 10 mg/mL solution of BrdU in PBS 2 h before sacrifice. Single-cell suspensions of IHLs were prepared 24 h after CCl_4 injection and stained for CD3 and NK1.1. Following the surface staining, the cells were fixed, stained for intracellular BrdU using a FITC-BrdU Flow kit (BD PharMingen) and analyzed by flow cytometry.

5,6-Carboxyfluoroscein succinimidyl ester (CFSE) staining

For isolation of NKT cells, the spleen was stained with anti-CD3-PE and anti-NK1.1-APC mAbs and sorted into $CD3^+/NK1.1^+$ (NKT) cells using a FACS Vantage instrument (Becton Dickinson, CA, USA). The isolated cells were re-suspended in PBS (1 × 105 cells/mL) containing 5-(and 6-) CFSE (Molecular Probes, OR, USA) at a final concentration of 1 μM, incubated at 37°C for 10 min, washed three times and co-incubated with murine recombinant IL-2 (10 U/mL) for 3 days in 96-well plates. The cells were then harvested and analyzed by FACS. Data analysis was performed using the FlowJo Software (Tree Star, CA, USA).

Cell culture and migration assay

The cell migration assay was performed using Multiwell 12-well plates (BD PharMingen). Immortalized liver endothelial cell line M1 cells from the liver of an H-2Kb-tsA58 transgenic mouse harboring the SV40 TAg gene were placed in the bottom wells.[28] Sorted NKT cells from CD44KO or WT mice were placed in the upper chambers of transwell inserts (pore size, 4 μm) and incubated with recombinant murine IL-2 (10 U/mL) at 37°C for 2 h. After incubation, the migrated cell numbers were quantified by MultiTox-Fluor Multiplex Cytotoxicity Assays (Promega, MI, USA).

Data analysis

All values in the figures and text are expressed as the mean ± SD. The significance of differences between mean values was evaluated by the Mann–Whitney *U*-test.

RESULTS

A single injection of CCl_4 induces NKT cell infiltration in CD44KO mice

TO DETERMINE WHETHER CD44 plays a role in liver injury, CD44KO and C57BL/6 WT mice (3 mice/group) were injected i.p. with CCl_4 (2.0 mL/kg body weight; 1 : 4 v/v in mineral oil) or mineral oil as a control. As shown in Figure 1a, similar sALT activities were detected in both types of treated mice after mineral oil injection (0 h). However, the sALT activity was significantly reduced in CD44KO mice at 6 h after CCl_4 injection. On the other hand, the sALT activities in CD44KO mice were significantly increased by about 1.5-fold at 12 and 24 h compared with WT mice.

Next, to determine the effects of CD44 on the infiltration of inflammatory cells in the same livers, we counted the absolute numbers of IHLs and calculated the number of cells in each IHL subset, as described previously.[10] As shown in Figure 1c, although the total number of IHLs was the same after mineral oil injection in CD44KO and WT mice, the numbers of IHLs were reduced in CD44KO mice at 2 and 6 h after CCl_4 injection compared with WT mice ($P < 0.05$), indicating that the absence of CD44 inhibited inflammatory cell infiltration into the liver within 6 h. However, consistent with the increased sALT activities, the total numbers of IHLs in CD44KO mice were significantly increased at 24 and 72 h. Interestingly, although most of the IHL phenotypes exhibited the same tendency to increase in total number, only the $CD3^+/NK1.1^+$ NKT cell population increased during the course of time recorded after CCl_4 injection (Fig. 1b,c). As shown in Figure 1b, the $CD3_+/NK1.1_+$ NKT cell subpopulation increased quickly within 6 h, compared with WT mice, and remained high until 24 h post-CCl_4 injection. It is worth noting that the $CD3_+/NK1.1_-$ T cells subpopulation in the liver of WT

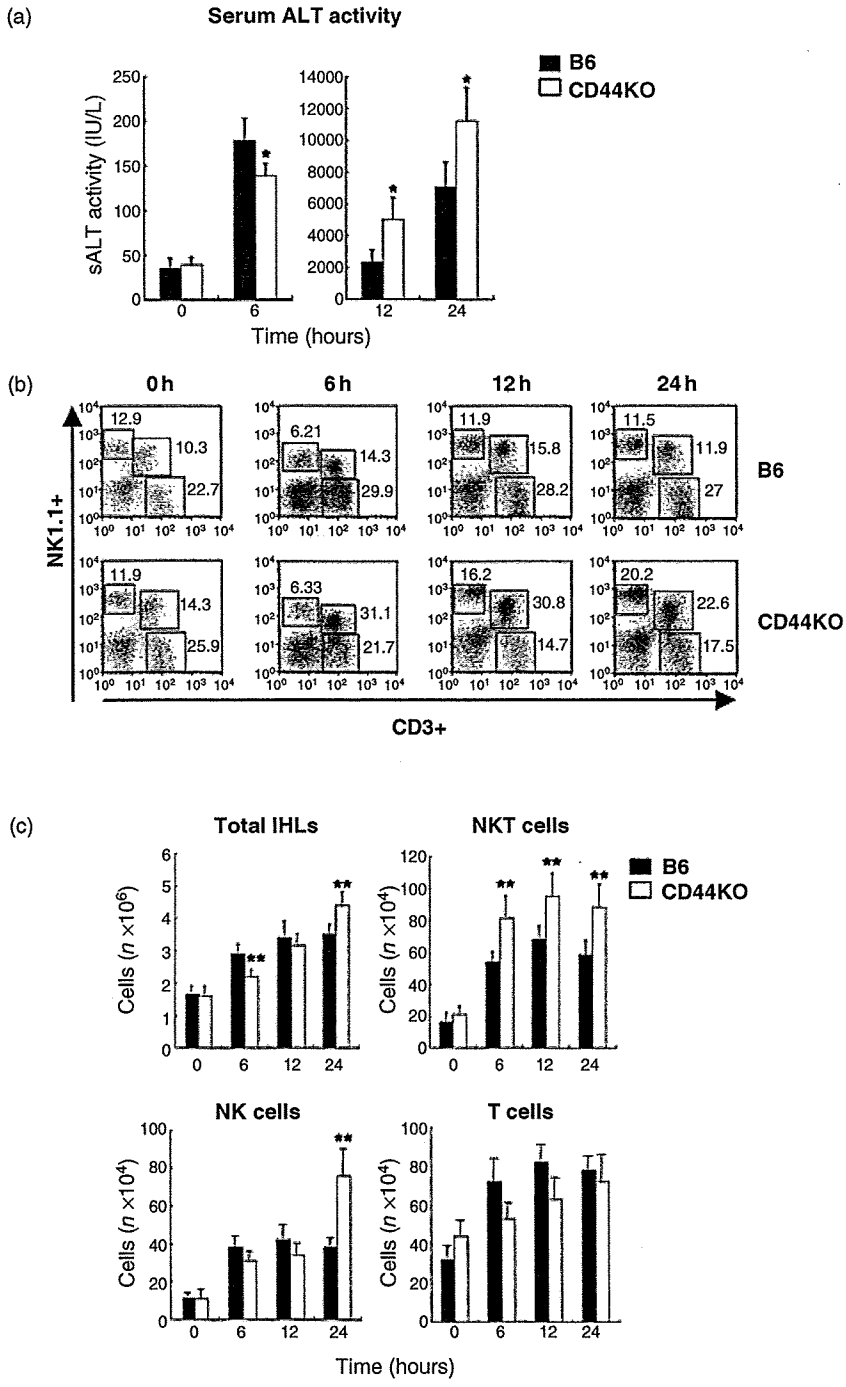

Figure 1 (a) Serum alanine aminotransferase (sALT) activity showing CD44KO mice with exacerbated liver injury after CCl_4 injection. Age-matched male CD44-deficient (CD44KO) and C57BL/6 mice (3 mice/group) were injected i.p. with a single dose of CCl_4 (2.0 mL/kg body weight; 1 : 4 v/v in mineral oil) and killed at the indicated time points. The mean sALT activity measured at the time of autopsy is indicated for each group and expressed in IU/L. (b) FACS analysis of intrahepatic leukocyte (IHL) cell subpopulations examined at 0, 6, 12 and 24 h after injection of CCL_4 or mineral oil as a control into C57BL/6 and CD44KO mice. IHLs were stained with anti-CD3-FITC and anti-NK1.1-PE monoclonal antibodies (mAbs) or anti-Gr-1-FITC and anti-CD11b-PE mAbs. Representative results of three independent experiments are shown. (c) IHLs were isolated from the mice and the effects of CD44 deficiency on cell recruitment were analyzed. The number of each subset of cells in the liver was calculated by multiplying the total number of IHLs by the frequency of each subset in the IHL population by FACS analysis (mean ± SD). $^*P < 0.05$ compared with C57BL/6 mice; $^{**}P < 0.05$.

mice were increased at 6 and 12 h after the injection, unlike the total IHL number.

As previously reported,[29] we found that the mRNA expression levels of inflammatory cytokines and chemokines in the liver showed the same kinetics as the sALT activities, meaning that CD44KO livers exhibited decreased expression at 6 h after CCl_4 injection but increased expression levels at 12 and 24 h compared with WT livers (data not shown). In particular, we found that MIP-2 mRNA expression was distinct, since MIP-2

mRNA expression was increased in CD44KO mouse livers at all the examined time points after CCl_4 injection.

Role of NKT cells

As described above, we found that NKT cells may play a critical role in liver injury in CD44KO mice after CCl_4 injection, as NKT cell migration was apparently increased compared with that of other inflammatory cells (see Fig. 1b,c). To evaluate the role of NKT cells in CD44KO mice, we generated double-KO mice for CD44 and NKT cells (CD44NKT DKO). CD44NKT DKO and CD44KO mice (5 mice/group) were injected i.p. with CCl_4 and killed at 6 and 24 h. As shown in Figure 2a, although there was no significant difference between the sALT activities at 6 h, CD44NKT DKO mice exhibited significantly lower sALT activity than CD44KO mice at 24 h ($P < 0.05$). Interestingly, these results revealed that NKT cells were not required for the early phase of liver injury by CCl_4 (6 h), since the sALT activities were similar with or without NKT cells. Based on the liver injury at 24 h, we found that the absolute numbers of total IHLs, macrophages and neutrophils among IHLs were significantly reduced in CD44NKT DKO mice (Fig. 2b,c). As shown in Figure 2d, consistent with the reduced number of macrophages in CD44NKT DKO mice, TNF-α mRNA expression was suppressed in the liver at 6 and 24 h after CCl_4 injection. Of note, hepatic MIP-2 mRNA expression in CD44NKT DKO mice was decreased at 6 h, indicating that NKT cells play an important role in MIP-2 production during this time. To support the RPA results, we confirmed that TNF-α production was reduced in the macrophages of CD44NKT DKO mice at 24 h relative to CD44KO mice (Fig. 2e).

Analysis of NKT cells

To address the reason why the number of NKT cells increased in CD44KO mice compared with WT mice, we proposed the following two hypotheses: (i) CD44KO NKT cells proliferate highly; and (ii) NKT cells migrate into the liver independent of the CD44 pathway. To examine the first hypothesis, we analyzed the proliferation of NKT cells using BrdU to determine the number of cells that had proliferated or were undergoing proliferation in the following experiments. CD44KO and WT mice were injected i.p. with 2 mg of BrdU 2 h before sacrifice. IHLs were isolated at 24 h after CCl_4 injection, subjected to BrdU labeling and then labeled with anti-mouse BrdU-FITC, CD3-PE and NK1.1-APC mAbs. As shown in Figure 3a, we found that $BrdU^+$ NKT cells were increased by about 10-fold in CD44KO mice compared to only 3-fold in WT mice after CCl_4 injection. To confirm this result, NKT cells were isolated from the liver by electronic sorting, subjected to CFSE staining and incubated with recombinant murine IL-2 (10 U/mL) for 3 days. Next, the co-cultures were harvested, and the percentage of proliferated NKT cells was determined by FACS analysis. As shown in Figure 3b, proliferation of NKT cells in the presence of recombinant IL-2 was greater for CD44KO mice than for WT mice, demonstrating that CD44KO NKT cells have the ability to strongly proliferate. However, there was no difference in the cytokine production levels of NKT cells after αGalCer stimulation in the presence or absence of CD44 (Fig. 3c). Further, we administered αGalcer (100 μg/kg) to the WT and CD 44KO mice, and analyzed sALT activity and the expression of the cytokine mRNA expression in the liver to confirm a difference in the activation of NKT cells by αGalcer in an *in vivo* system. Interestingly, we found sALT activity in CD44KO mice also increased at 24 h compared with WT mice after αGalcer injection (Supporting Information 1).

In vitro migration assays revealed that isolated NKT cells from CD44KO and WT mice showed similar migration toward liver sinus endothelial cell (LSEC) line cells (Fig. 3d). Immunohistochemical analysis suggested that adhesion between NKT cells and LSEC line cells was observed at similar ratios in the two strains of mice, indicating that NKT cell migration was not dependent on the CD44 pathway (Fig. 3e).

Roles of cytokines and chemokines

To evaluate which cytokines or chemokines are responsible for liver injury, we performed antibody neutralization experiments. Groups of 3 CD44KO mice were injected (250 μg/mouse) with anti-IFN-γ mAb, anti-TNF-α mAb, anti-MIP-2 mAb or rat IgG prior to injection of CCl_4, and killed after 24 h. As shown in Figure 4a, treatment with anti-MIP-2 mAb significantly protected against the increase in sALT activity, indicating that MIP-2 plays a key role in liver injury. Consistent with the results for the sALT activity and to a lesser extent than anti-MIP-2 mAb administration, anti-TNF-α mAb administration decreased the number of total IHLs after CCl_4 injection. Further, anti-MIP-2 mAb treatment reduced all phenotypes among the IHLs, indicating that MIP-2 is responsible for cell infiltration as well as liver injury.

Importantly, neutralization of MIP-2 reduced intrahepatic expression of TNF-α mRNA, suggesting that MIP-2

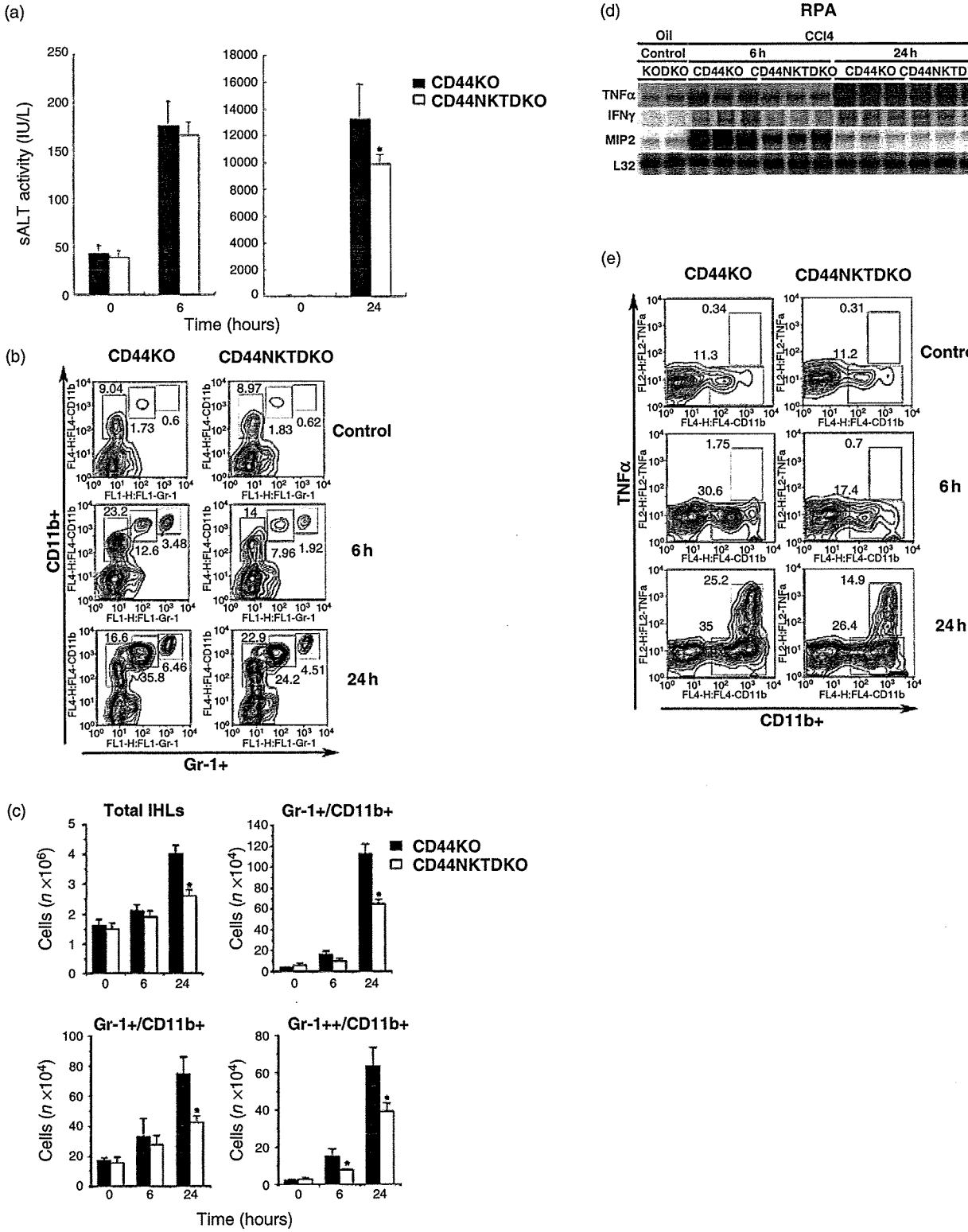

Figure 2 The role of natural killer T (NKT) cells. (a) Serum alanine aminotransferase (sALT) activity in 10 age-matched 8–11-week-old male CD44NKT DKO and CD44KO mice injected with CCl_4 and killed at 6 or 24 h. (b–c) FACS analysis of three animals in both groups. Intrahepatic leukocytes (IHLs) were isolated and stained with anti-Gr-1-FITC and anti-CD11b-APC monoclonal antibodies (mAbs). Representative results of three independent experiments are shown and the absolute cell numbers were calculated. (d) Total hepatic RNA (20 μg) was isolated from livers at the indicated time points and analyzed for cytokine and chemokine expressions by ribonuclease protection assay. (e) Intracellular cytokine expression of macrophages. IHLs were stained with anti-mouse Gr-1-FITC, CD11b-APC and TNF-α-PE mAbs and analyzed using a FACSCalibur system.

production triggers the expression of other inflammatory cytokine cascades (Fig. 4c). Consistent with the cytokine profiles, neutralization of MIP-2 and TNF-α effectively diminished the induction of hepatocyte apoptosis (Fig. 4d) as well as the necrotic parenchymal changes around the periportal vein.

Role of CD44 in the liver fibrosis model

To evaluate whether CD44 deficiency affects chronic liver injury as well as acute liver injury, groups of 3 CD44NKT DKO, CD44KO and WT mice were injected i.p. with CCl_4 twice per week.

Initially, we measured the sALT activity at 24 h after the first injection every week and found that the sALT activity in CD44KO mice was elevated compared with those in CD44NKT DKO and WT mice (Fig. 5a). To address the degree of liver fibrosis in the presence or absence of CD44, we analyzed the liver histology using AZAN staining and immunohistochemistry with an anti-αSMA antibody. As shown in Figure 5c, there was a significant difference between the αSMA-positive areas in CD44KO and WT mice, suggesting that CD44KO mice exhibited enhanced liver fibrosis. On the other hand, immunohistochemical staining for PCNA, a marker for the G_1/S phase of the cell cycle, was used to determine whether the absence of CD44 caused abnormal hepatocyte proliferation after injury. The numbers of PCNA-positive hepatocytes in CD44KO livers were increased, but not significantly, compared to those in WT livers after 2 and 4 weeks of CCl_4 injections. Further, as shown in Figure 5b, intrahepatic expression of TGF-β1 mRNA was apparently increased in the liver of CD44KO mice compared with that of WT mice. However, we could not find a difference between the matrix metallo proteinase (MMPs) and tissue inhibitor of metalloproteinase (TIMPs) family expression in the liver between CD44KO and WT mice. Interestingly, we found that CD44NKT DKO mice exhibited a reduction in the area of liver fibrosis after calculation of the AZAN- and αSMA-positive areas, revealing that NKT cells have an effector function against hepatocytes under CD44-deficient conditions.

DISCUSSION

IN THE PRESENT study, we demonstrated that CD44 has dual effects on liver inflammation using a CCl_4-induced liver injury model. It has already been reported that anti-CD44 antibody treatment for pulmonary eosinophilia,[30] rheumatoid arthritis[31] and experimental encephalomyelitis[32] reduces the inflammatory response by suppressing the migration of inflammatory cells into the inflamed tissue. In contrast, however, CD44KO mice are reported to exhibit exacerbation of *bleomycin-* or *Escherichia coli*-induced lung injury via induction of cell apoptosis in the parenchyma and infiltration of neutrophils in the lung.[15,17] The reason for this contradiction remains unknown. Here, we showed several interesting findings with regards to CD44 and liver inflammatory response using CCl_4.

First, we found that only the population of NKT cells was increased in the liver after CCl_4 treatment, while other cell populations showed reduced numbers during the early phase. Importantly, NKT cells derived from CD44KO mice exhibited higher proliferative activities after CCl_4 treatment compared with those from WT mice, since CFSE- or BrdU-positive NKT cells were increased in our *ex vivo* and *in vivo* systems. It has been demonstrated that liver lymphomononuclear cells from CD44KO mice are highly proliferative in the staphylococcal enterotoxin B-induced liver injury model.[33] Further, we previously showed that IHLs from CD44KO mice were more resistant to apoptosis than those from WT mice at 24 h after CCl_4 treatment.[29] Since IHLs are highly proliferative and resistant to apoptosis in CD44KO mice, theoretically, all cell subpopulations would be expected to increase. However, we found that only NKT cells increased. Based on these results, we conclude that the main mechanism for the increase in CD44KO NKT cells is that NKT cells can adhere to

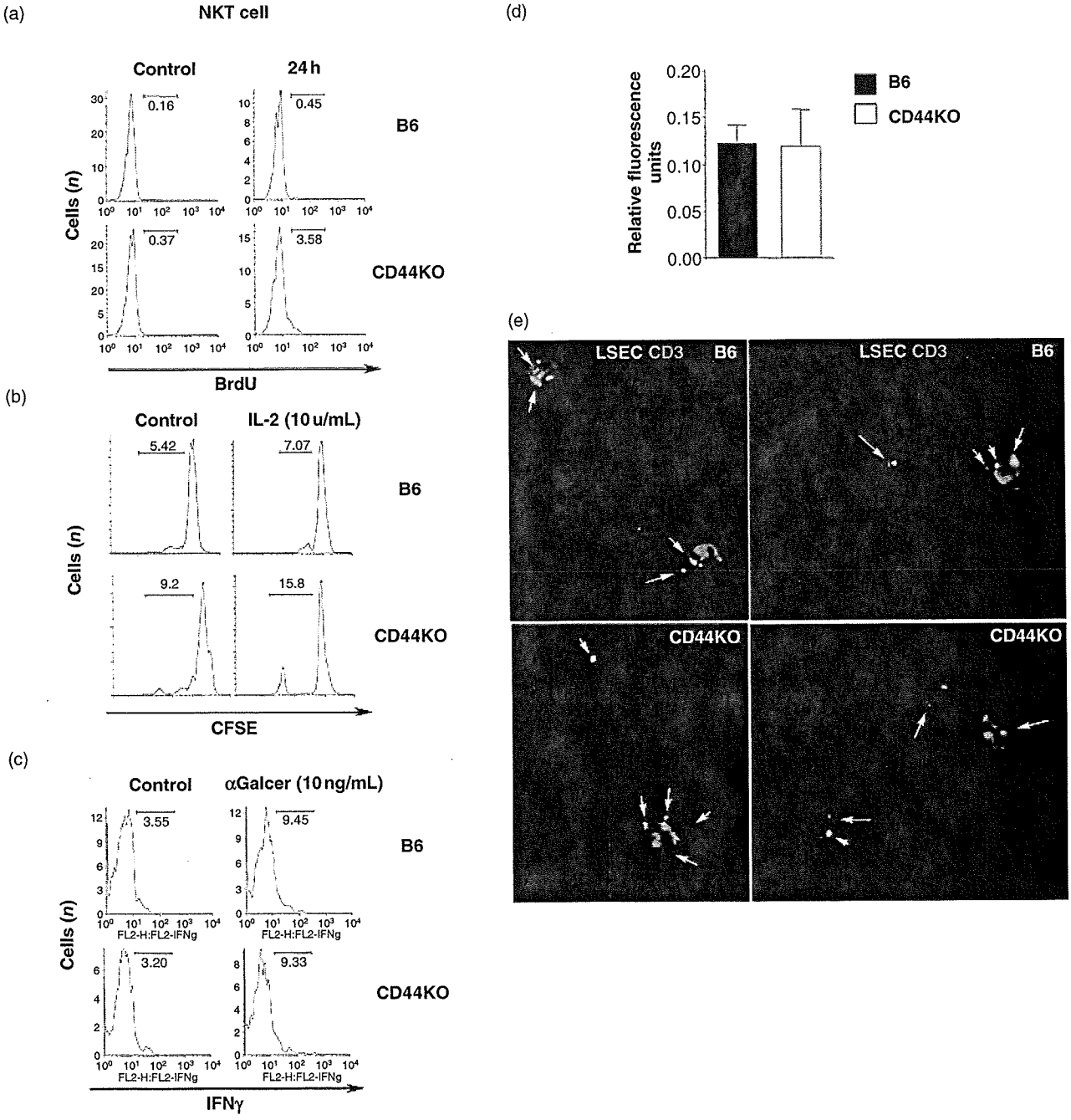

endothelial cells without utilizing the CD44 pathway. In support of this hypothesis, cell migration assays between isolated NKT cells and LSEC line cells revealed that NKT cells migrated toward to the LSEC line cells at similar levels regardless of the presence or absence of CD44. Recent reports have demonstrated that NKT cells express high levels of LFA-1, which is thought to be required for the development and/or survival of liver NKT cells.[23,24] These results suggest that the major adhesion molecule on NKT cells for infiltration into the liver may be LFA-1 through its interaction with CD54. Although we confirmed the expression of LFA-1 on NKT

Figure 3 Proliferation of intrahepatic leukocytes (IHLs) is higher in CD44KO mice than in wild type (WT) mice. (a) *In vivo*: CD44KO and WT mice were injected i.p. with 2 mg of BrdU at 2 h before sacrifice. IHLs were isolated at 24 h after CCl_4 injection, subjected to BrdU labeling and then labeled with anti-mouse BrdU-FITC, CD3-PE and NK1.1-APC monoclonal antibodies (mAbs). Data shown are representative of triplicate mice. (b) *In vitro*: After isolating IHLs from CD44KO and WT mice, IHLs were isolated using a fluorescence-activated cell sorter (FACS) sorting system, stimulated with recombinant IL-2 (10 U/mL) for 72 h and analyzed for CFSE dye loss by FACS analysis. Data are representative of 3–6 independent experiments. (c) *In vitro*: After isolating IHLs from CD44KO and WT mice, the cells were cultured with αGalCer (10 ng/mL) for 4 h and then labeled with anti-CD3-FITC, anti-NK1.1-APC and anti-IFN-γ-PE mAbs. Representative results of three independent experiments are shown. (d) Migration assay of immortalized liver endothelial cells (M1 cells). Sorted NKT cells (labeled with anti-CD3-PE and anti-NK1.1-APC mAbs) from CD44KO and WT mice were placed in the upper chambers of transwell inserts and incubated with recombinant murine IL-2 (10 U/mL) at 37°C for 2 h. After the incubation, the numbers of migrated cells in the lower chambers were quantified by MultiTox-Fluor Multiplex Cytotoxicity Assay. (e) The migrated cells from CD44KO and WT mice in the lower chambers were stained with FITC-LSEC and observed by light microscopy to determine their immunohistochemistry.

cells from CD44KO and WT mice, there was no difference in the expression levels (data not shown).

Second, we found that expression of MIP-2 mRNA was elevated in the liver at 6 h after CCl_4 treatment. Despite the increased expression of major inflammatory cytokines and chemokines in WT mice compared with CD44KO mice, only the expression of MIP-2 showed different patterns at this time point. Consistent with a recent report,[34] we also found that expression of MIP-2 was reduced in CD44NKT DKO mice compared with CD44KO mice, suggesting that NKT cells may produce MIP-2 in the liver after CCl_4 treatment. It is noteworthy to mention that these results may depend on the reduced numbers of macrophages and neutrophils due to the absence of NKT cells, since we have already shown that depletion of macrophages causes reduced expression of MIP-2 in the liver.[29] Although such a scenario is possible, we suggest that NKT cells from CD44KO mice were the main producers of MIP-2 and that this chemokine triggered the migration of other inflammatory cells into the liver. This scenario is supported by our findings that anti-MIP-2 mAb treatment decreased the sALT activity, inflammatory cell migration and induction of hepatocyte apoptosis in the liver.

MIP-2 has been identified as being functionally analogous to human IL-8 and is produced by macrophages, monocytes, fibroblasts and endothelial cells.[35,36] Some reports have suggested that MIP-2 is involved in the liver injury after hepatic ischemia-reperfusion and in the Con A-induced hepatitis model.[37–39] Thus, we conclude that induction of MIP-2 release from NKT cells and macrophages in CD44KO mice causes migration of other cells into the liver and, as a consequence, reinforces liver inflammation.

We found that CD44KO mice exhibited exacerbated liver fibrosis after repeated CCl_4 injections. This is the first evidence that CD44 is involved in the formation of liver fibrosis. These results suggest that CD44 not only contributes to acute liver injury but also to chronic liver damage. Although we have not shown the results obtained with hepatic stellate cells (HSCs), which are key players in liver fibrosis[40,41] we found that HSCs expressed CD44 and that the number of HSCs was increased in CD44KO mice compared with WT mice at day 7 after CCl_4 injection. It is curious that adhesion molecules, such as CD44, are involved in the formation of liver fibrosis and this represents a novel finding. This might be a candidate for target therapy for liver fibrosis.

In summary, we have shown that inhibition of CD44 has dual effects on liver inflammation. In the liver, CD44 deficiency induced suppression of cell recruitment (except NKT cells) and protected against liver inflammation due to decreased expression of inflammatory cytokines during the early phase. However, despite the suppressed cell recruitment, NKT cells still migrated to the liver in a CD44-independent manner and were highly proliferative. NKT cells induced MIP-2 expression in the liver and, in turn, this chemokine triggered the late phase and severe liver inflammation with increased hepatocyte apoptosis via the NF-κB signaling pathway. Thus, caution is warranted for the protection of the liver immune system when using the adhesion molecule CD44 as a therapeutic target for inflammatory liver diseases.

ACKNOWLEDGMENTS

WE ARE GRATEFUL to Dr. Tak. W. Mak (University of Toronto) for providing the CD44KO mice. We are also grateful to Dr. Toshinori Nakayama (Chiba University) and Dr. Masaru Taniguchi (RIKEN) for providing the Vα14 NKT-KO mice. We thank Tomomi Saeki

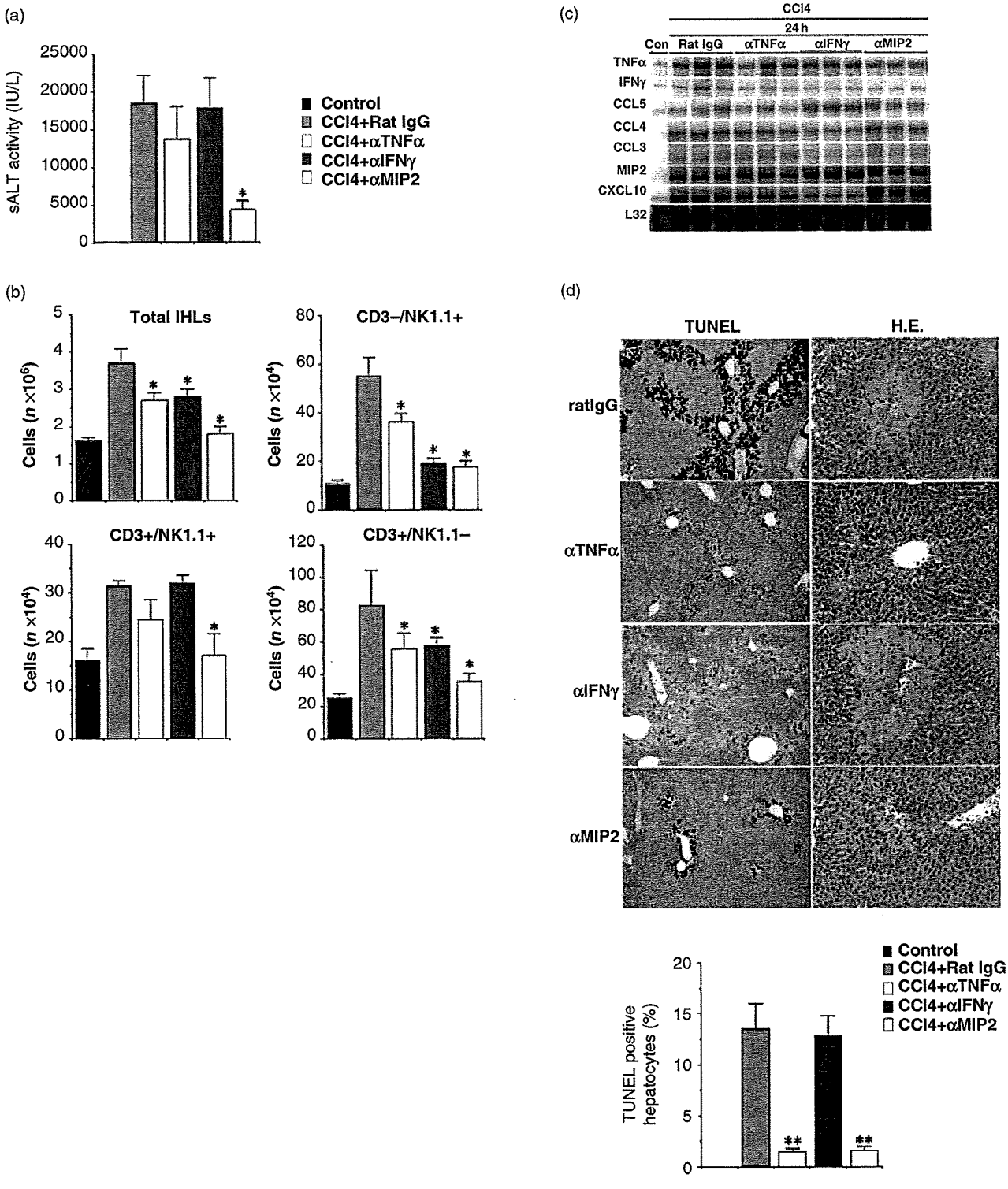

Figure 4 (a) Age-matched male CD44KO mice were injected with anti-IFN-γ monoclonal antibody (mAb) (250 μg), anti-TNF-α mAb (250 μg), anti-MIP-2 mAb (250 μg) or control rat IgG prior to injection with CCl_4 to determine serum alanine aminotransferase (sALT) activity. (b) Intrahepatic leukocytes (IHLs) from five groups of three mice were isolated and stained with anti-CD3-FITC and anti-NK1.1-APC mAbs or anti-Gr-1-FITC and anti-CD11b-APC mAbs. Representative results of three independent experiments are shown and the absolute cell numbers were calculated. (c) Total hepatic RNA (20 μg) was isolated from livers at various time points and analyzed for cytokine and chemokine expression by ribonuclease protection assay (RPA). (d) To evaluate the induction of apoptosis, liver sections were stained using the in situ terminal deoxynucleotidyl transferase nick end-labeling (TUNEL) assay (6). The percentages of apoptotic hepatocytes among the total hepatocytes were determined by TUNEL staining. Data are expressed as the mean ± SD for three mice. $*P < 0.05$; $**P < 0.01$.

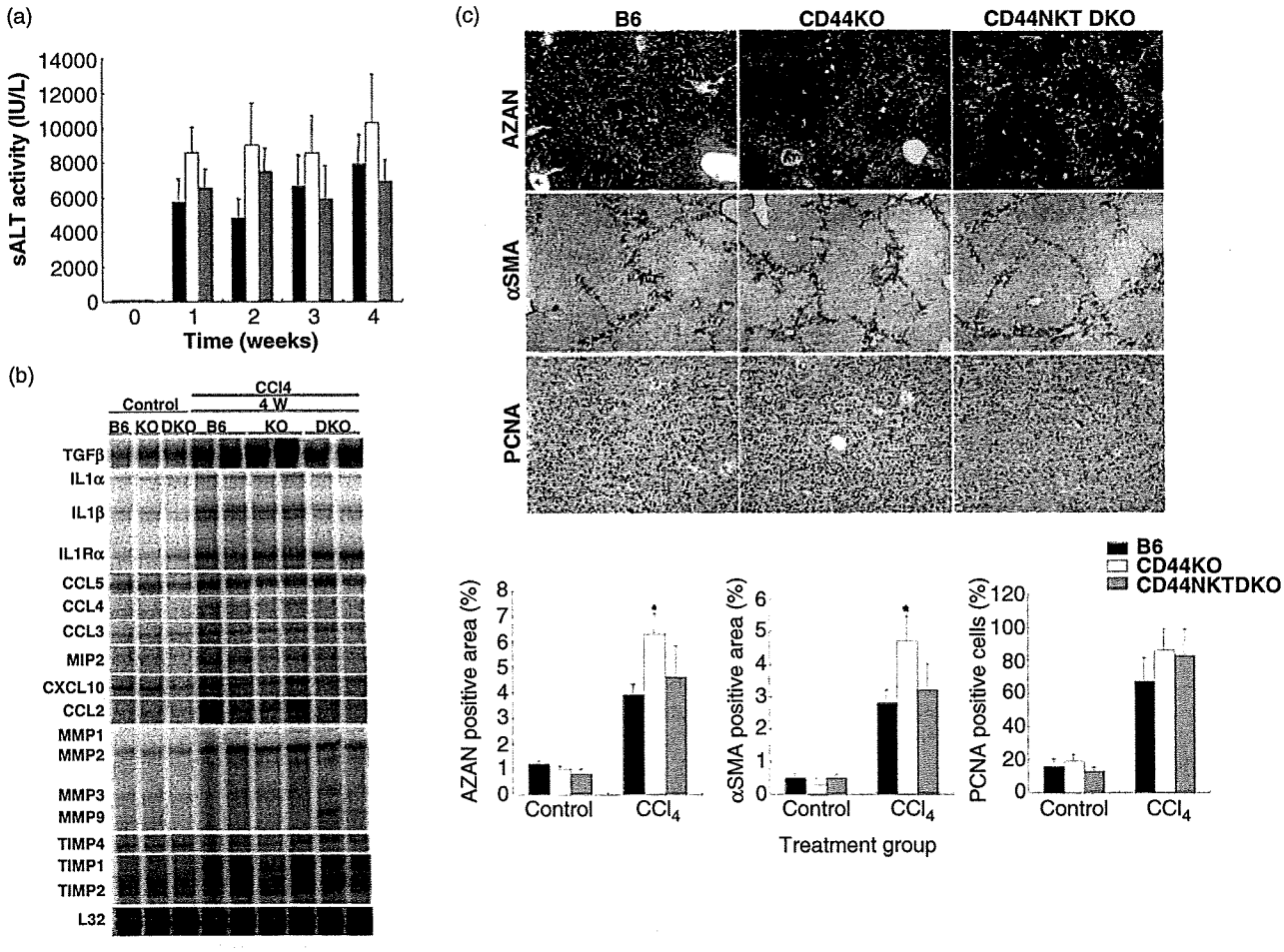

Figure 5 Liver fibrosis model. (a) CD44NKT DKO, CD44KO and C57BL/6 mice were injected i.p. with CCl_4 twice per week for 4 weeks and serum alanine aminotransferase (sALT) activity was measured at 24 h after the second injection. The mice were killed at 4 weeks. (b) Total hepatic RNA (20 μg) was isolated from livers at various time points and analyzed for the expression of cytokines, matrix metallo proteinase (MMPs) and tissue inhibitor of metalloproteinase (TIMPs) by ribonuclease protection assay (RPA). (c) Liver sections were obtained from mice killed after 4 weeks of repeated CCl_4 injections and stained with AZAN and an anti-αSMA monoclonal antibody (mAb) for evaluation of liver fibrosis. Immunohistochemical staining for PCNA, a marker for the G_1/S phase of the cell cycle, was used to determine whether the absence of CD44 caused abnormal hepatocyte proliferation after CCl_4 injections. The percentages of liver fibrosis were determined by the numbers of αSMA-positive cells or the AZAN-stained areas. Data are expressed as the mean ± SD for three mice. $*P < 0.05$.

and Yumiko Okuda for mice experiments. We thank Kirin Brewery for providing the αGalCer (KRN7000). This study was supported by Grants-in-Aid (B) from the Ministry of Education, Culture, Sports, Science and Technology of Japan (Grant No. 87100000183) and a Grant from the Tokai Science Academy to Kimura K.

REFERENCES

1 Crispe IN. Hepatic T cells and liver tolerance. *Nat Rev Immunol* 2003; **3**: 51–62.
2 Peters M, Vierling J, Gershwin ME, Milich D, Chisari FV, Hoofnagle JH. Immunology and the liver. *Hepatology* 1991; **13**: 977–94.
3 Guidotti LG, Chisari FV. Noncytolytic control of viral infections by the innate and adaptive immune response. *Annu Rev Immunol* 2001; **19**: 65–91.
4 Wardle EN. Kupffer cells and their function. *Liver* 1987; **7**: 63–75.
5 Yoneyama H, Matsuno K, Zhang Y *et al.* Regulation by chemokines of circulating dendritic cell precursors, and the formation of portal tract-associated lymphoid tissue, in a granulomatous liver disease. *J Exp Med* 2001; **193**: 35–49.
6 Knolle PA, Schmitt E, Jin S *et al.* Induction of cytokine production in naive CD4(+) T cells by antigen- presenting murine liver sinusoidal endothelial cells but failure to induce differentiation toward Th1 cells. *Gastroenterology* 1999; **116**: 1428–40.
7 Guidotti LG, Rochford R, Chung J, Shapiro M, Purcell R, Chisari FV. Viral clearance without destruction of infected cells during acute HBV infection. *Science* 1999; **284**: 825–9.
8 Kakimi K, Guidotti LG, Koezuka Y, Chisari FV. Natural killer T cell activation inhibits hepatitis B virus replication in vivo. *J Exp Med* 2000; **192**: 921–30.
9 Kimura K, Kakimi K, Wieland S, Guidotti LG, Chisari FV. Activated intrahepatic antigen-presenting cells inhibit hepatitis B virus replication in the liver of transgenic mice. *J Immunol* 2002; **169**: 5188–95.
10 Kimura K, Moriwaki H, Nagaki M *et al.* Pathogenic role of B cells in anti-CD40-induced necroinflammatory liver disease. *Am J Pathol* 2006; **168**: 786–95.
11 Lee WY, Kubes P. Leukocyte adhesion in the liver: distinct adhesion paradigm from other organs. *J Hepatol* 2008; **48**: 504–12.
12 Springer TA. Traffic signals for lymphocyte recirculation and leukocyte emigration: the multistep paradigm. *Cell* 1994; **76**: 301–14.
13 Springer TA. Traffic signals on endothelium for lymphocyte recirculation and leukocyte emigration. *Annu Rev Physiol* 1995; **57**: 827–72.
14 Siegelman MH, Stanescu D, Estess P. The CD44-initiated pathway of T-cell extravasation uses VLA-4 but not LFA-1 for firm adhesion. *J Clin Invest* 2000; **105**: 683–91.
15 Teder P, Vandivier RW, Jiang D *et al.* Resolution of lung inflammation by CD44. *Science* 2002; **296**: 155–8.
16 Vachon E, Martin R, Plumb J *et al.* CD44 is a phagocytic receptor. *Blood* 2006; **107**: 4149–58.
17 Wang Q, Teder P, Judd NP, Noble PW, Doerschuk CM. CD44 deficiency leads to enhanced neutrophil migration and lung injury in Escherichia coli pneumonia in mice. *Am J Pathol* 2002; **161**: 2219–28.
18 Seino K, Taniguchi M. Functionally distinct NKT cell subsets and subtypes. *J Exp Med* 2005; **202**: 1623–6.
19 Taniguchi M, Harada M, Kojo S, Nakayama T, Wakao H. The regulatory role of Valpha14 NKT cells in innate and acquired immune response. *Annu Rev Immunol* 2003; **21**: 483–513.
20 Cui J, Shin T, Kawano T *et al.* Requirement for Valpha14 NKT cells in IL-12-mediated rejection of tumors. *Science* 1997; **278**: 1623–6.
21 Kawano T, Cui J, Koezuka Y *et al.* CD1d-restricted and TCR-mediated activation of valpha14 NKT cells by glycosylceramides. *Science* 1997; **278**: 1626–9.
22 Kawano T, Cui J, Koezuka Y *et al.* Natural killer-like nonspecific tumor cell lysis mediated by specific ligand-activated Valpha14 NKT cells. *Proc Natl Acad Sci USA* 1998; **95**: 5690–3.
23 Emoto M, Mittrucker HW, Schmits R, Mak TW, Kaufmann SH. Critical role of leukocyte function-associated antigen-1 in liver accumulation of CD4+NKT cells. *J Immunol* 1999; **162**: 5094–8.
24 Matsumoto G, Kubota E, Omi Y, Lee U, Penninger JM. Essential role of LFA-1 in activating Th2-like responses by alpha-galactosylceramide-activated NKT cells. *J Immunol* 2004; **173**: 4976–84.
25 Matsumoto G, Omi Y, Lee U, Nishimura T, Shindo J, Penninger JM. Adhesion mediated by LFA-1 is required for efficient IL-12-induced NK and NKT cell cytotoxicity. *Eur J Immunol* 2000; **30**: 3723–31.
26 Schmits R, Filmus J, Gerwin N *et al.* CD44 regulates hematopoietic progenitor distribution, granuloma formation, and tumorigenicity. *Blood* 1997; **90**: 2217–33.
27 Kimura K, Nagaki M, Takai S, Satake S, Moriwaki H. Pivotal role of nuclear factor kappaB signaling in anti-CD40-induced liver injury in mice. *Hepatology* 2004; **40**: 1180–9.
28 Matsuura T, Kawada M, Hasumura S *et al.* High density culture of immortalized liver endothelial cells in the radial-flow bioreactor in the development of an artificial liver. *Int J Artif Organs* 1998; **21**: 229–34.
29 Kimura K, Nagaki M, Kakimi K *et al.* Critical role of CD44 in hepatotoxin-mediated liver injury. *J Hepatol* 2008; **48**: 952–61.
30 Katoh S, Matsumoto N, Kawakita K, Tominaga A, Kincade PW, Matsukura S. A role for CD44 in an antigen-induced murine model of pulmonary eosinophilia. *J Clin Invest* 2003; **111**: 1563–70.
31 Brocke S, Piercy C, Steinman L, Weissman IL, Veromaa T. Antibodies to CD44 and integrin alpha4, but not

L-selectin, prevent central nervous system inflammation and experimental encephalomyelitis by blocking secondary leukocyte recruitment. *Proc Natl Acad Sci USA* 1999; 96: 6896–901.
32 Mikecz K, Brennan FR, Kim JH, Glant TT. Anti-CD44 treatment abrogates tissue oedema and leukocyte infiltration in murine arthritis. *Nat Med* 1995; 1: 558–63.
33 McKallip RJ, Fisher M, Gunthert U, Szakal AK, Nagarkatti PS, Nagarkatti M. Role of CD44 and its v7 isoform in staphylococcal enterotoxin B-induced toxic shock: CD44 deficiency on hepatic mononuclear cells leads to reduced activation-induced apoptosis that results in increased liver damage. *Infect Immun* 2005; 73: 50–61.
34 Diao H, Kon S, Iwabuchi K *et al.* Osteopontin as a mediator of NKT cell function in T cell-mediated liver diseases. *Immunity* 2004; 21: 539–50.
35 Broxmeyer HE, Sherry B, Lu L *et al.* Enhancing and suppressing effects of recombinant murine macrophage inflammatory proteins on colony formation in vitro by bone marrow myeloid progenitor cells. *Blood* 1990; 76: 1110–16.
36 Tekamp-Olson P, Gallegos C, Bauer D *et al.* Cloning and characterization of cDNAs for murine macrophage inflammatory protein 2 and its human homologues. *J Exp Med* 1990; 172: 911–19.
37 Halder RC, Aguilera C, Maricic I, Kumar V. Type II NKT cell-mediated anergy induction in type I NKT cells prevents inflammatory liver disease. *J Clin Invest* 2007; 117: 2302–12.
38 Jaeschke H. Molecular mechanisms of hepatic ischemia-reperfusion injury and preconditioning. *Am J Physiol Gastrointest Liver Physiol* 2003; 284: G15–26.
39 Jaeschke H. Mechanisms of liver injury. II. Mechanisms of neutrophil-induced liver cell injury during hepatic ischemia-reperfusion and other acute inflammatory conditions. *Am J Physiol Gastrointest Liver Physiol* 2006; 290: G1083–8.
40 Friedman SL. Seminars in medicine of the Beth Israel Hospital, Boston. The cellular basis of hepatic fibrosis. Mechanisms and treatment strategies. *N Engl J Med* 1993; 328: 1828–35.
41 Friedman SL. Molecular regulation of hepatic fibrosis, an integrated cellular response to tissue injury. *J Biol Chem* 2000; 275: 2247–50.

Supporting Information

The following Supporting Information can be found in the online version of the article:

Supporting Information 1. Materials and Methods. *aGalCer injection in vivo. Serum ALT activity.*

Please note: Wiley-Blackwell are not responsible for the content or functionality of any supporting information supplied by the authors. Any queries (other than missing material) should be directed to the corresponding author for the article.

Role of TNF-α Produced by Nonantigen-Specific Cells in a Fulminant Hepatitis Mouse Model

Hiroyasu Ito,[1]* Kazuki Ando,*‡ Tetsuya Ishikawa,§ Kuniaki Saito,*¶ Masao Takemura,* Michio Imawari,‖ Hisataka Moriwaki,† and Mitsuru Seishima*

In previous studies, the mechanisms of acute liver injury and virus exclusion have been examined using a model wherein HBsAg-specific CTL are injected into HBsAg transgenic (Tg) mice. The importance of the role of TNF-α in virus exclusion was shown, but its role in liver injury was unclear. We crossed the TNF-α knockout mouse and HBsAg-Tg mouse to establish the HBsAg-Tg/TNF-α KO mouse, and examined the influence of TNF-α on liver injury. The severity of liver damage, as determined by serum alanine aminotransferase activity, was ~100 times greater in HBsAg-Tg/TNF-$\alpha^{+/+}$ than in HBsAg-Tg/TNF-$\alpha^{-/-}$ mice after i.v. administration of 5 × 10^6 CTLs. This liver damage reached the peak of its severity within 24–48 h, and was restored 7 days later. Histopathological examination showed hepatocellular necrosis and inflammatory cell infiltrate 24 h after the CTL injection in HBsAg-Tg/TNF-$\alpha^{+/+}$ mice but not in HBsAg-Tg/TNF-$\alpha^{-/-}$ mice. The liver damage was fatal for all HBsAg-Tg/TNF-$\alpha^{+/+}$ mice that received 1.5 × 10^7 CTLs. In contrast, 1.5 × 10^7 CTLs could not kill the HBsAg-Tg/TNF-$\alpha^{-/-}$ mice. The TNF-α production level was enhanced after the CTL injection in not only intrahepatic macrophages but also other types of mononuclear cells from non-HBsAg-Tg/TNF-$\alpha^{+/+}$ mice. An adoptive transfer examination revealed that severe liver damage occurred in HBsAg-Tg/TNF-$\alpha^{-/-}$ mice that had received mononuclear cells from TNF-$\alpha^{+/+}$ mice. In conclusion, the present study provides evidence that TNF-α produced by intrahepatic non-Ag-specific inflammatory cells is critical in the development of lethal necroinflammatory liver disease. *The Journal of Immunology,* **2009, 182: 391–397.**

Hepatitis B virus (HBV)[2] is a nonlytic virus that does not directly infect cells and cause damage. Liver damage and viral clearance after an HBV infection are thought to be mediated by the host's cellular immune response to viral Ags (1). $CD8^+$ CTL play a critical role in the liver damage and viral clearance in HBV infections. These effector functions include the secretion of cytokines, such as IFN-γ and TNF-α, as well as cytolytic activity mediated by perforin and granzyme B (2–5). HBsAg transgenic (Tg) mice show no symptoms of liver disease until the adoptive transfer of HBsAg-specific CTLs, after which they develop a necroinflammatory liver disease that is histologically similar to acute viral hepatitis in man (6). The first step, which begins within 1 h of CTL administration, involves Ag recognition by the CTLs and delivery of a signal that results in the death of the hepatocyte. In the second step, which begins in 4–12 h, the CTLs recruit many host-derived inflammatory cells in their immediate vicinity, resulting in the formation of necroinflammatory foci. The third step is detectable 24–72 h after CTL administration: the livers display massive hepatocellular necrosis and an inflammatory cell infiltrate that consists principally of host-derived mononuclear cells and pronounced sinusoidal lining cell hyperplasia, which resembles the histopathological changes observed in patients dying from liver failure due to HBV-induced fulminant hepatitis. Using this murine fulminant hepatitis model, various studies have been conducted on viral clearance and liver disease in HBV infection.

TNF-α production is one of the earliest events in many types of liver injuries, and it triggers the production of other cytokines that together recruit inflammatory cells, kill hepatocytes, and initiate a hepatic healing response that includes fibrogenesis. The serum levels of TNF-α are significantly increased in patients with fulminant hepatitis (7). In viral hepatitis, elevated levels of plasma TNF-α and soluble TNFR are frequently observed (8). TNF-α is known to be released mainly by macrophages, but it also released by $CD4^+$ and $CD8^+$ T, B, NK (9), and dendritic cells (10). In particular, recent studies have shown that TNF-α is also released by CTLs (3) and contributes to CTL-mediated cytotoxicity, although its cytolytic activity is not as high as those of perforin and the Fas ligand (11–13).

The role of TNF-α is important not only in virus exclusion, but also in liver injury. However, in this model, it is considered that many host-derived inflammatory cells recruited by CTLs are critical in massive hepatocellular necrosis. In the present study, we crossed the TNF-α knockout (TNF-$\alpha^{-/-}$) mouse with the HBsAg-Tg mouse, to establish the HBsAg-Tg/TNF-$\alpha^{-/-}$ mouse, and examined the influence of TNF-α produced by non-Ag-specific inflammatory cells on liver injury in a murine viral fulminant hepatitis model.

Materials and Methods

Mice

Male B10.D2 (H-2^d) mice (age, 6–8 wk; weight, 25–30 g) were obtained from Japan SLC. The HBsAg-Tg mice lineage 107-5D (official designation

*Department of Informative Clinical Medicine and †First Department of Internal Medicine, Gifu University Graduate School of Medicine, Gifu City, Japan; ‡Goto Clinic, Ohgaki City, Gifu Prefecture, Japan; §Cancer Immunotherapy Center, Nagoya Kyoritsu Hospital, Nakagawa, Nagoya, Japan; ¶Human Health Sciences, Graduate School of Medicine and Faculty of Medicine, Kyoto University, Shogoin, Sakyo, Kyoto, Japan; and ‖Second Department of Internal Medicine, Showa University School of Medicine, Shinagawa-ku, Tokyo, Japan

Received for publication November 27, 2007. Accepted for publication November 3, 2008.

The costs of publication of this article were defrayed in part by the payment of page charges. This article must therefore be hereby marked *advertisement* in accordance with 18 U.S.C. Section 1734 solely to indicate this fact.

[1] Address correspondence and reprint requests to Dr. Hiroyasu Ito, Department of Informative Clinical Medicine, Gifu University Graduate School of Medicine, 1-1 Yanagido, Gifu, Japan. E-mail address: hito@gifu-u.ac.jp

[2] Abbreviations used in this paper: HBV, hepatitis B virus; Tg, transgenic; sALT, serum alanine aminotransferase; MNC, mononuclear cell.

Tg (Alb-1, HBV) Bri66; inbred B10.D2, H-2^d), in which the HBV envelope coding region is under the control of the mouse albumin promoter, was provided by Dr. F. V. Chisari (Department of Molecular and Experimental Medicine, The Scripps Research Institute, La Jolla, CA). TNF-$\alpha^{-/-}$ mice were produced by gene targeting as described previously (14) and backcrossed onto B10.D2 (H-2^d). HBsAg-Tg/TNF-$\alpha^{-/-}$ mice were produced by backcrossing TNF-$\alpha^{-/-}$ mice with 107-5D.

Cell lines and reagents

P815 cells expressing HBV-preS1, 2, and S (P815preS1), and HBsAg-specific, $CD8^+$ CTL clones (6C2) were provided by Dr. F. V. Chisari (Department of Molecular and Experimental Medicine, The Scripps Research Institute, La Jolla, CA). The clones are H-2d restricted, and can recognize an epitope (IPQSLDSWWTSL) located between residues 28 and 39 of HBsAg. Five days after the last stimulation with irradiated P815preS1, the cells were washed and injected i.v. into HBsAg-Tg mice. (However, the phenotype of the 6C2, which we used in the present study, was changed in cytokines production. Therefore, we termed it 6C2-08.) Recombinant murine IFN-γ was obtained from R&D Systems.

Disease model

Five days after the last stimulation, the 6C2-08 cells were washed three times, suspended in PBS, and injected i.v. into HBsAg-Tg, non-Tg and HBsAg-Tg/TNF-$\alpha^{-/-}$ recipients. Hepatocellular injury was monitored biochemically by measuring serum alanine aminotransferase (sALT) activity. At appropriate time points, mice were killed by cervical dislocation and necropsy was performed. Tissue samples were fixed in 10% formalin, embedded in paraffin, and sectioned; the sections were then stained with H&E. The intrahepatic distribution of HBV Ags was assessed by the indirect immunoperoxidase method using 3-amino-9-ethyl carbazole.

Preparation of hepatic mononuclear cells and hepatocytes

Hepatic mononuclear cells (MNCs) (15) and hepatocytes (16) were isolated using the described simplified technique. The liver was perfused with liver perfusion and digestion medium (Life Technologies). Hepatocytes were separated from the MNCs by centrifugation at 50 × *g* for 2 min and were washed twice in complete RPMI 1640 (Nikken Biomedical Laboratory). MNC populations were purified using M-SMF (JINRO).

Real-time PCR

Total RNA was isolated and transcribed into cDNA using an RNeasy Mini Kit and an Omniscript Reverse Transcriptase Kit (Qiagen GmbH). The resulting cDNA was used as a template for real-time PCR along with primer/probe sets for TNF-α, TNFR1, and TNFR2 (TaqMan Gene Expression Assays; Applied Biosystems) and 2× TaqMan Universal PCR Master Mix (Applied Biosystems), according to the manufacturer's recommendations. The primer/probe sets for 18S were used as an internal control in each reaction (Applied Biosystems). Real-time PCR data were analyzed using the sequence detector software (Applied Biosystems).

TNF-α detection by ELISA

Macrophages, NK cells, CD4 T cells, and CD8 T cells were obtained from intrahepatic MNCs of HBsAg-Tg/TNF-$\alpha^{+/+}$ mice treated with 6C2 cells with the help of an immunomagnetic separation system (MACS System), and cultured for 24 h. The concentrations of TNF-α in the culture supernatant were determined by an enzyme-linked absorbent assay kit for TNF-α (R&D Systems), according to the manufacturer's instruction. The experimental results are expressed as the mean of triplicates ± SD of three independent experiments.

Intracellular cytokine staining

For intracellular staining, the hepatic MNCs from the mice that were administered 6C2 cells were incubated for 4 h with brefeldin A (10 μg/ml). Then, these cells were fixed, permeabilized the Cytofix/Cytoperm buffer (BD Pharmingen), and stained with FITC-conjugated anti-mouse TNF-α (clone MP6-XT22; eBioscience). Samples were acquired on a FACStar flow cytometer and data analysis was conducted using the CellQuest software (BD Pharmingen).

Adoptive cell transfer

HBsAg-Tg/TNF-$\alpha^{-/-}$ mice received CD4-positive splenocytes, CD8-positive splenocytes, DX5-positive splenocytes, and CD11b-positive splenocytes as well as non-CD4, non-CD8, non-DX5, and non-CD11b splenocytes (8 × 10^6/mouse), which were isolated by MACS from the non-HBsAg-Tg/TNF-$\alpha^{+/+}$ mice 7 days before the CTL injection. To confirm the existence of the transferred cells, we labeled the isolated cells with CFSE and performed flow cytometric analysis. Approximately 4% of IHLs were CFSE positive at 7 days after the injection. Hepatocellular injury was monitored biochemically by measuring the sALT activity.

Statistics

Values are expressed as means ± SEM. Differences between the experimental and control groups were analyzed by the Kruskal-Wallis test followed by Scheffe's F test. Significance was established at $p < 0.05$.

Results

Induction of fulminant hepatitis by HBsAg-specific CTLs in HBsAg-Tg/TNF-$\alpha^{+/+}$ mice, but not in HBsAg-Tg/TNF-$\alpha^{-/-}$ mice

CTL clones 6C2-08 (1×10^6) were incubated with 1×10^6 irradiated stimulator cells (P815-preS1) in complete medium without EL-4 supernatant. 6C2-08 were collected 12 h after stimulation and analyzed for IFN-γ and TNF-α mRNA expression by 6C2-08 (Fig. 1*A*). The IFN-γ and TNF-α mRNA expression was enhanced in 6C2-08 after stimulation. HBsAg-Tg/TNF-$\alpha^{+/+}$ and HBsAg-Tg/TNF-$\alpha^{-/-}$ mice received a single i.v. injection of CTLs (5×10^6 cells/mouse). As shown in Fig. 1*B*, severe liver damage (as determined by the sALT levels) was observed in HBsAg-Tg/TNF-$\alpha^{+/+}$ mice that were administered CTLs, but not in HBsAg-Tg/TNF-$\alpha^{-/-}$ or non-HBsAg-Tg/TNF-$\alpha^{+/+}$ mice. Histological changes in the livers of HBsAg-Tg/TNF-$\alpha^{+/+}$, HBsAg-Tg/TNF-$\alpha^{-/-}$, and non-HBsAg-Tg/TNF-$\alpha^{+/+}$ mice were examined on days 2 and 5 after the CTL injection. A histological analysis revealed widely scattered necroinflammatory foci, containing mostly mononuclear cells and apoptotic hepatocytes in the livers of HBsAg-Tg/TNF-$\alpha^{+/+}$ mice after the CTL injection (Fig. 1*C*). In contrast, in HBsAg-Tg/TNF-$\alpha^{-/-}$ mice, invasion of a large amount of inflammatory cells and hepatocellular necrosis were not observed. Next, to confirm the HBsAg expression in hepatocytes after the CTL injection, we stained the liver tissues with anti-HBsAg mAb 5 days after the CTL injection. Immunohistopathological examination revealed that HBsAg expression in the hepatocytes of HBsAg-Tg/TNF-$\alpha^{+/+}$ mice was down-regulated compared with that of HBsAg-Tg/TNF-$\alpha^{-/-}$ mice.

CTL dose-dependent induction of liver disease and mortality in HBsAg-Tg/TNF-$\alpha^{+/+}$ and HBsAg-Tg/TNF-$\alpha^{-/-}$ mice

Disease severity was also strictly dependent on the CTL dose in the HBsAg-Tg/TNF-$\alpha^{-/-}$ recipient mice (Fig. 2*A*). Liver damage was detectable biochemically at CTL doses above 1.5×10^6 CTLs per mouse in the HBsAg-Tg/TNF-$\alpha^{-/-}$ mice. The resultant liver damage (as determined by the sALT levels) at a high dose (1.5×10^7 CTLs per mouse) was not severe enough to be fatal (1900 ± 187 IU/L). In contrast, in HBsAg-Tg/TNF-$\alpha^{+/+}$ mice, the liver damage was severe enough to be fatal within 96 h in two of six recipients (33.3%) who were administered 0.8×10^7 HBsAg-specific CTLs, and it was fatal for all seven mice (100%) that received 1.5×10^7 CTLs (Fig. 2*B*).

TNF-α production by hepatic macrophages, NK cells, CD4 T cells, and CD8 T cells in HBsAg-Tg/TNF-$\alpha^{+/+}$ mice after the CTL injection

As shown in from several publications (7, 17), patients with fulminant hepatitis have increased serum TNF-α levels. Therefore, we next isolated macrophages, NK cells, CD4 T cells, and CD8 T cells from the intrahepatic MNCs of HBsAg-Tg/TNF-$\alpha^{+/+}$ mice that had received HBsAg-specific CTLs by immunomagnetic separation and examined which cell fractions produced TNF-α. Twenty-four hours after the CTL injection, the TNF-α mRNA expression was enhanced in all the cell fractions, and it was decreased

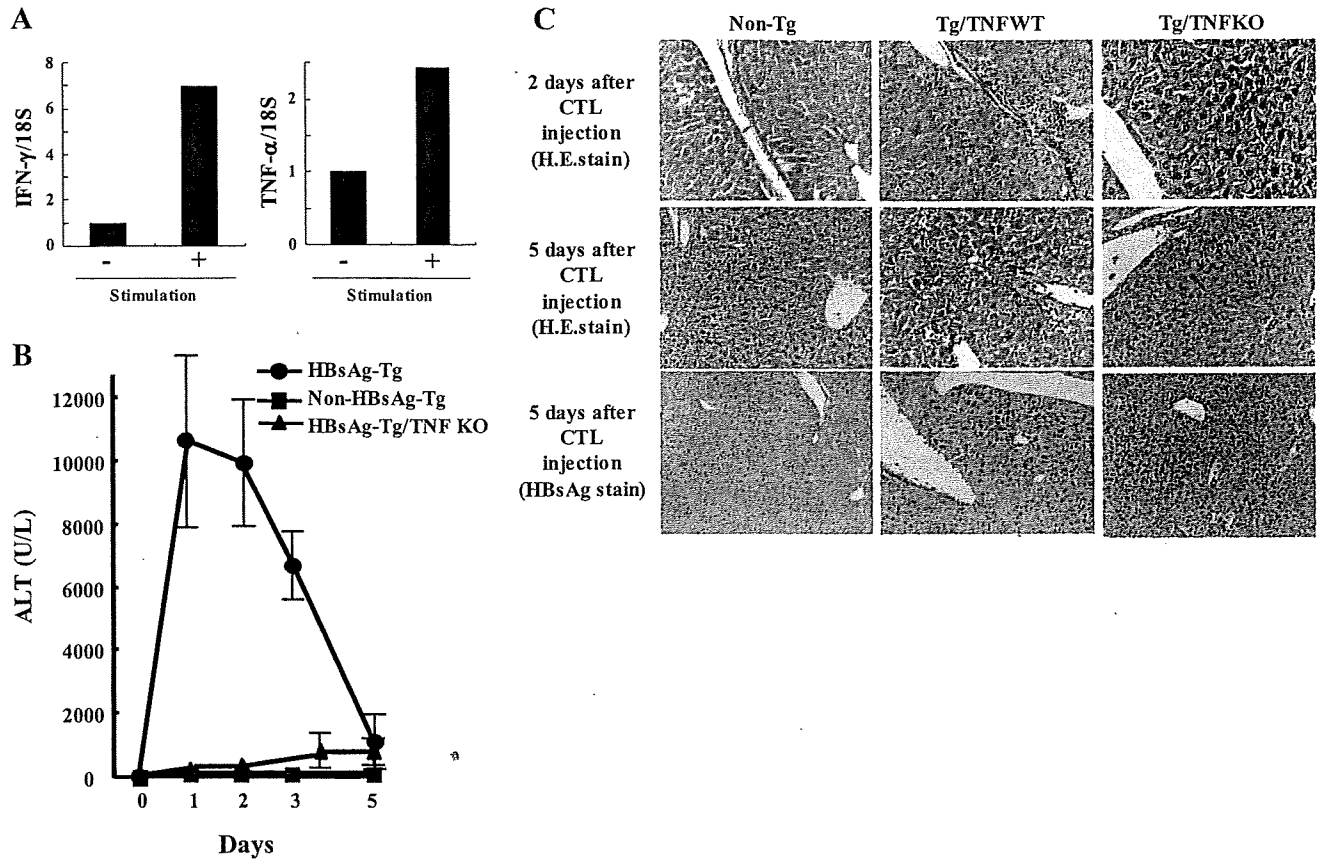

FIGURE 1. CTL-induced liver disease in HBsAg-Tg/TNF-$\alpha^{+/+}$ and HBsAg-Tg/TNF-$\alpha^{-/-}$ mice. *A*, CTL clones 6C2-08 (1×10^6) were incubated with 1×10^6 irradiated stimulator cells (P815-preS1) in complete medium without EL-4 supernatant. 6C2-08 were collected 12 h after stimulation and analyzed for IFN-γ and TNF-α mRNA expression by 6C2-08. *B*, Serum ALT activity was analyzed at varying time points relative to the injection of 5×10^6 HBsAg-specific CTLs into groups of three HBsAg-Tg/TNF-$\alpha^{+/+}$ mice, HBsAg-Tg/TNF-$\alpha^{-/-}$ mice, and non-HBsAg-Tg/TNF-$\alpha^{+/+}$ mice. *C*, Histopathological characteristics of HBsAg-Tg/TNF-$\alpha^{+/+}$ mice and HBsAg-Tg/TNF-$\alpha^{-/-}$ mice livers observed at 2 and 5 days (hematoxylin and eosin, ×200) after CTL administration in these mice. The intrahepatic HBsAg content was demonstrated by immunohistochemical staining for HBsAg in the lower panel.

48 h after the CTL injection (Fig. 3*A*). Next, we measured the TNF-α protein production levels in hepatic MNCs after the administration of HBsAg-specific CTLs by ELISA and intracellular cytokine staining. As shown in Fig. 3*B*, the level of TNF-α secreted by CD11b-positive cells and DX5-positive cells from HBsAg-Tg/TNF-$\alpha^{+/+}$ mice treated with CTLs was increased

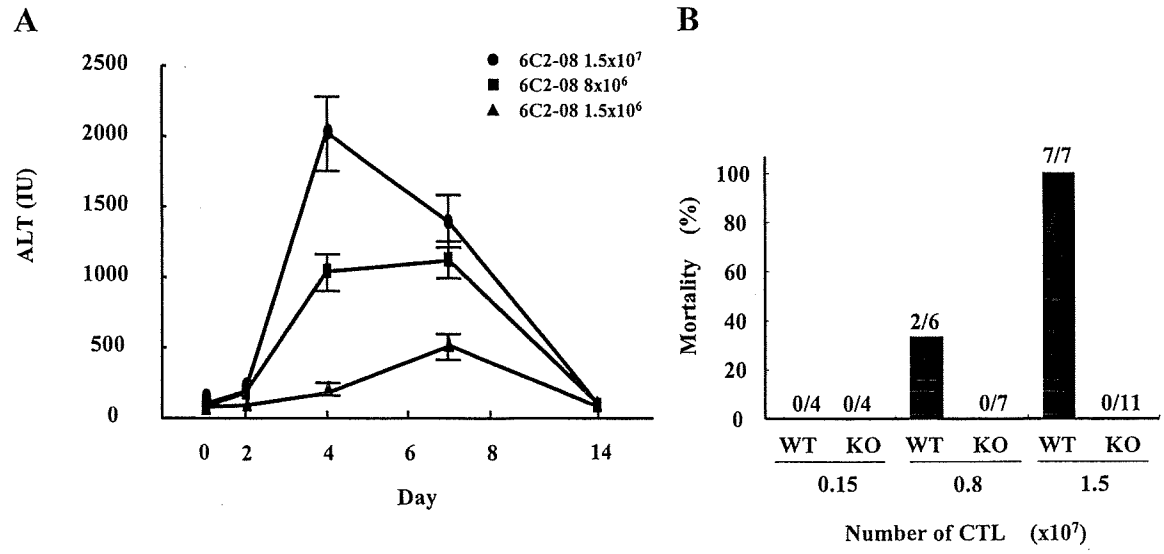

FIGURE 2. CTL-induced liver disease and mortality depended on the number of CTLs administered in HBsAg-Tg/TNF-$\alpha^{+/+}$ and HBsAg-Tg/TNF-$\alpha^{-/-}$ mice. *A*, Serum ALT activity was monitored at 0, 2, 4, 6, 8, and 14 days after the injection of varying doses of HBsAg-specific CTLs into HBsAg-Tg/TNF-$\alpha^{-/-}$ mice. *B*, The results reflect the mortality after i.v. injection of 1.5×10^6, 8×10^6, and 1.5×10^7 CTLs into HBsAg-Tg/TNF-$\alpha^{+/+}$ and HBsAg-Tg/TNF-$\alpha^{-/-}$ mice.

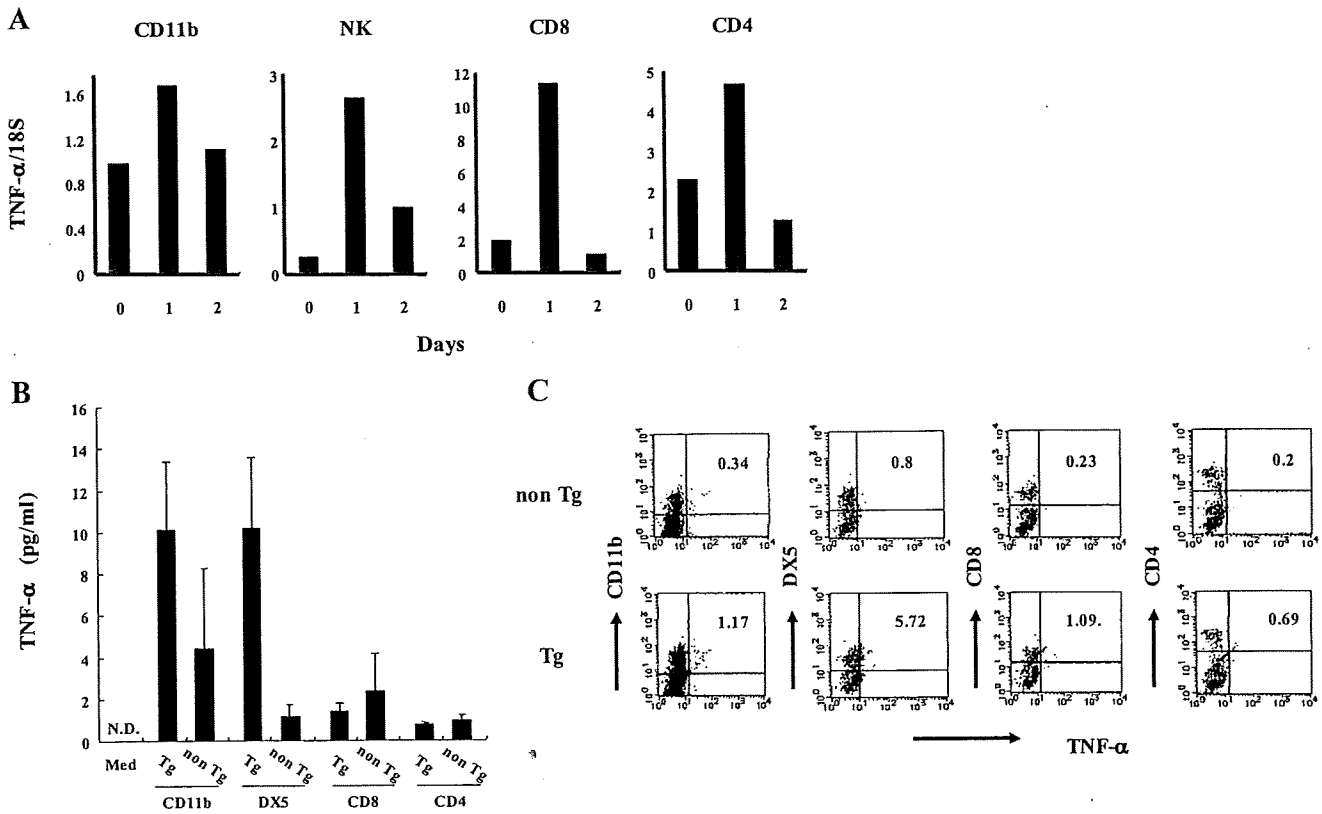

FIGURE 3. TNF-α production by intrahepatic CD11b$^+$, NK$^+$, CD8$^+$, and CD4$^+$ cells from HBsAg-Tg/TNF-α$^{+/+}$ mice that were administered HBsAg-specific CTLs. *A*, TNF-α mRNA expression by intrahepatic CD11b$^+$, NK$^+$, CD8$^+$, and CD4$^+$ cells from HBsAg-Tg/TNF-α$^{+/+}$ mice that were administered CTLs. Hepatic CD11b$^+$, NK$^+$, CD8$^+$, and CD4$^+$ cells were purified with the MACS system (purity of each cell fraction, >95%). The mRNA levels for TNF-α were normalized to that of 18S mRNA. Representative charts derived from the analyses of three mice per group. *B*, Hepatic CD11b$^+$, NK$^+$, CD8$^+$, and CD4$^+$ cells from HBsAg-Tg/TNF-α$^{+/+}$ mice that were administered HBsAg-specific CTLs were purified by the MACS system. These cells were cultured for 24 h. TNF-α concentrations in the culture supernatants were measured by ELISA. *C*, Flow cytometric analysis for intracellular TNF-α produced by hepatic CD11b$^+$, NK$^+$, CD8$^+$, and CD4$^+$ cells obtained from mice 24 h after the injection of CTLs and cultured for 4 h in brefeldin A.

compared with those from non HBsAg-Tg mice. However, CD8-positive cells and CD4-positive cells from HBsAg-Tg/TNF-α$^{+/+}$ mice treated with CTLs did not produce TNF-α. The intracellular staining results indicated that TNF-α production in CD11b-positive, DX5-positive, CD8-positive cells, and CD4-positive cells from HBsAg-Tg/TNF-α$^{+/+}$ mice increased after the CTL injection (Fig. 3*C*).

Role of TNF-α-producing non-Ag-specific cells

The requirement of TNF-α-producing cells for the development of hepatitis was further evaluated with the help of experiments involving the adoptive transfer of macrophages, NK cells, CD4 T cells, and CD8 T cells from non-HBsAg-Tg/TNF-α$^{+/+}$ mice into HBsAg-Tg/TNF-α$^{-/-}$ mice. HBsAg-Tg/TNF-α$^{-/-}$ recipient mice were administered 1.5 × 10^7 HBsAg-specific CTLs 5 days after the i.v. injection of freshly isolated macrophages, NK cells, CD4 T cells, and CD8 T cells from TNF-α$^{+/+}$ mice. We confirmed the existence of the CFSE-labeled transferred cells by flow cytometric analysis (data not shown). As shown in Fig. 4, the sALT levels several days after the CTL injection were significantly increased in HBsAg-Tg/TNF-α$^{-/-}$ mice pretreated with of isolated macrophages, NK cells, CD4 T cells, and CD8 T cells from TNF-α$^{+/+}$ mice compared with the sALT levels in non-pretreated HBsAg-Tg/TNF-α$^{-/-}$ mice.

Effect of IFN-γ on HBsAg-Tg/TNF-α$^{+/+}$ and HBsAg-Tg/TNF-α$^{-/-}$ mice

IFN-γ and TNF-α were thought to be critical components in this murine fulminant hepatitis model (6). We examined the direct effect of IFN-γ on HBsAg-Tg/TNF-α$^{+/+}$ and HBsAg-Tg/TNF-α$^{-/-}$ mice. As shown in Fig. 5*A*, recombinant murine IFN-γ administration caused marked elevations in sALT activity in the HBsAg-Tg/TNF-α$^{+/+}$ compared with in the HBsAg-Tg/TNF-α$^{-/-}$

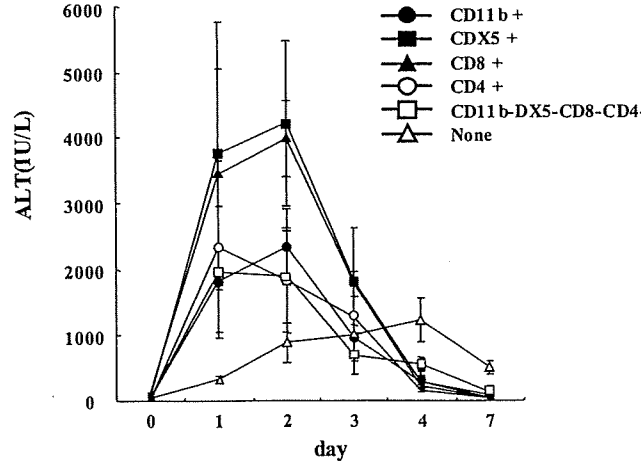

FIGURE 4. MACS-sorted CD11b$^+$, NK$^+$, CD8$^+$, and CD4$^+$ cells from TNF-α$^{+/+}$ mice were transferred i.v. into HBsAg-Tg/TNF-α$^{-/-}$ mice 5 days before injection of the HBsAg-specific CTLs (1.5 × 10^7/mouse). The number of transferred cells was 8 × 10^6/mouse. Serum ALT activities were assessed at the indicated days after the CTL injection. Each value is represented by the mean ± SEM of three mice.

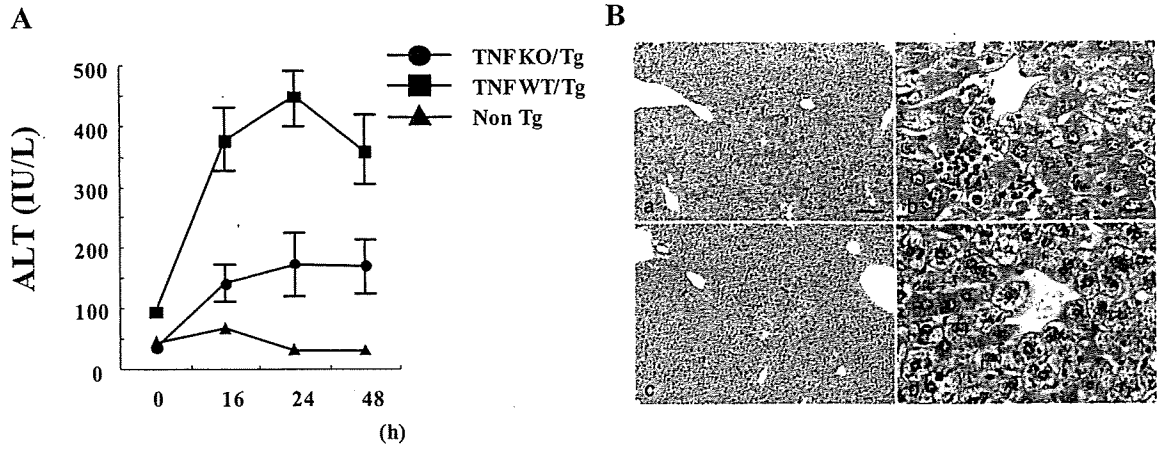

FIGURE 5. Kinetics of recombinant murine IFN-γ-induced liver injury in HBsAg-Tg/TNF-$\alpha^{+/+}$ and HBsAg-Tg/TNF-$\alpha^{-/-}$ mice. Groups of five HBsAg-Tg/TNF-$\alpha^{+/+}$ mice, matched HBsAg-Tg/TNF-$\alpha^{-/-}$ mice, and non-HBsAg-Tg/TNF-$\alpha^{+/+}$ mice were i.v. administered recombinant IFN-γ (8000 U/mouse). *A*, The serum ALT levels were measured at 0, 16, 24, and 48 h after the recombinant IFN-γ injection. Each value is represented by the mean ± SEM of three mice. *B*, Histopathological examination of HBsAg-Tg/TNF-$\alpha^{+/+}$ mice and matched HBsAg-Tg/TNF-$\alpha^{-/-}$ mice livers observed at 24 h after the recombinant murine IFN-γ administration in these mice. *a* and *b*, HBsAg-Tg/TNF-$\alpha^{+/+}$ mice. *c* and *d*, HBsAg-Tg/TNF-$\alpha^{-/-}$ mice. *a* and *c*, Low-power field of liver tissue. *b* and *d*, High-power field of liver tissue. Scale bars: 100 μm (*a*) and 25 μm (*b*). Yellow arrowheads, small necroinflammatory foci; blue arrows, apoptotic hepatocytes.

mice. In contrast, recombinant murine TNF-α administration caused a similar elevation in sALT activity in the HBsAg-Tg/TNF-$\alpha^{+/+}$ and HBsAg-Tg/TNF-$\alpha^{-/-}$ mice, but it did not enhance the sALT levels in non-HBsAg-Tg mice (data not shown). Histopathological examination revealed the presence of small necroinflammatory foci and apoptotic hepatocytes in the liver of HBsAg-Tg/TNF-$\alpha^{+/+}$ mice after the administration of recombinant IFN-γ; however, these changes were not observed in the liver of HBsAg-Tg/TNF-$\alpha^{-/-}$ mice (Fig. 5*B*).

Kinetics of hepatocyte TNFR mRNA expression in HBsAg-Tg/TNF-$\alpha^{+/+}$ mice after the CTL injection

Next, we tested the TNFR 1 and 2 mRNA expressions in hepatocytes after the CTL injection. The expression of TNFR 1 mRNA in hepatocytes in the HBsAg-Tg/TNF-$\alpha^{+/+}$ mice was obviously enhanced (more than 40-fold) after the CTL injection and peaked 24 h thereafter (Fig. 6). In contrast, the expression of TNFR 2 mRNA in hepatocytes in the HBsAg-Tg/TNF-$\alpha^{+/+}$ mice was unchanged after the CTL injection.

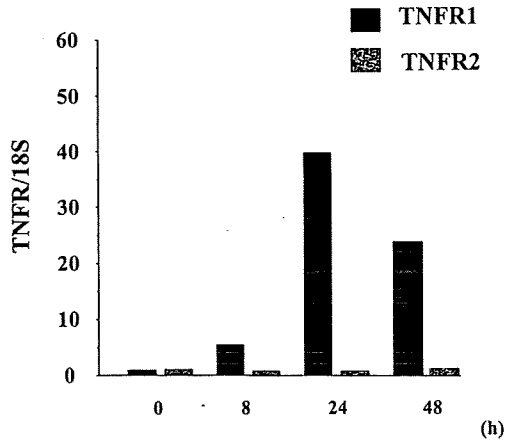

FIGURE 6. Kinetics of TNFR mRNA expression on hepatocytes in HBsAg-Tg/TNF-$\alpha^{+/+}$ mice that were administered HBsAg-specific CTLs. Hepatocytes were collected by perfusion from HBsAg-Tg/TNF-$\alpha^{+/+}$ mice at the indicated times after the CTL injection. Levels of TNFR1 and TNFR2 mRNA were normalized to that of 18S mRNA. The data expressed are relative to the findings from untreated HBsAg-Tg/TNF-$\alpha^{+/+}$ mice. The representative charts are derived from the analyses of three mice per group.

Discussion

Fulminant hepatitis is a clinical syndrome consisting of sudden and severe liver injury that results in hepatic encephalopathy and acute liver failure (17, 18). The rate of mortality from fulminant hepatitis remains very high, although intensive medical care and implementation of the latest therapies, including liver transplantation, are progressing. The HBsAg-Tg mouse model contributed to the study on the mechanisms of fulminant hepatitis (4, 6). Previously, various reports provided HBV transgenic mice. The HBsAg transgenic mouse lineage 107-5D, lineage pFC80-219, or HBV transgenic mouse lineage 1.3.32 were suitable for examining CTL-induced hepatitis (19). Lethal fulminant hepatitis was only observed when the HBsAg transgenic mouse lineage 107-5D received HbsAg specific CTL clones. In lineage pFC80–219 and lineage 1.3.32 HBV Tg mice, lethal hepatitis was not caused by the high-dose CTL injection. Recently, many reports have discussed the influence of the genotypes on outcome of HBV infections. It was reported that the intracellular accumulation of HBV DNA and Ags may play a role in inducing liver damage (20). Moreover, HBV/genotype Bj was an independent risk factor for the development of fulminant hepatitis, and the expression of intracellular Ags in HBV/genotype Bj was the highest (20, 21). Therefore, the HBsAg transgenic mouse lineage 107-5D may be suitable for the analysis of human fulminant hepatitis because the HBsAg particles were retained within the endoplasmic reticulum of the hepatocyte in this lineage. However, it is thought that the HBsAg transgenic mouse lineage 107-5D should be used only for the analysis of the fulminant hepatitis and not acute hepatitis or chronic hepatitis. Previous studies have described the relative hierarchy of the perforin-granzyme, FasL-Fas, IFN-γ, and TNF-α death pathways in the pathogenesis of the necroinflammatory liver disease induced by HBsAg-specific CTL clones in HBsAg transgenic mice (3, 6). Kondo et al. (22) demonstrated that liver injury was attenuated by blocking the FasL-Fas and TNF-α-TNFR pathway in the fulminant hepatitis model. In contrast, it was reported that IFN-γ-dependent signals are primarily responsible for killing HBsAg-positive hepatocytes irrespective of the presence or absence of FasL and Fas. Moreover,

hepatocytes are much less sensitive to destruction by TNF-α than by the other death pathways in the fulminant hepatitis model (3). This discrepancy remains unsolved. However, the difference might be due to the difference in the methods used to block the FasL and Fas signaling. Nakamoto et al. (3) used Fas and FasL knockout mice for blocking the signaling. In contrast, the use of the soluble form of Fas has also been reported. We previously reported that anti-TNF-α Abs were only modestly protective against CTL-induced liver disease. In contrast, Kondo et al. (22) appropriated soluble TNFRβ-Fc for the TNF-TNFR blocking experiment. TNFRβ-Fc greatly inhibited the increase in the ALT level in the fulminant hepatitis model. Thus, in the present study, we examined the role of TNF-α using TNF-α knockout mice. The proinflammatory cytokine TNF-α is thought to play a critical role in acute viral hepatitis (7, 8, 23).We established the HBsAg-Tg (lineage 107-5D)/TNF-$\alpha^{-/-}$ mouse strain and have shown that TNF-α secreted by intrahepatic non-Ag-specific inflammatory cells plays a critical role in the development of acute and lethal necroinflammatory liver disease.

TNF-α is a pleiotropic cytokine that induces cellular responses such as proliferation, production of inflammatory mediators, and cell death, and plays a major role in the pathogenesis of septic shock and wasting syndrome. In the liver, TNF-α is involved in the pathophysiology of viral hepatitis, alcoholic liver disease, nonalcoholic fatty liver disease, and ischemia-reperfusion injury. TNF-α plays a dichotomous role in the liver, where it not only acts as a mediator of cell death but also induces hepatocyte proliferation and liver regeneration. In particular, in HBV-related acute hepatitis, TNF-α is thought to contribute to the viral clearance and development of the necroinflammatory liver disease. It was reported that mice that express HBV envelope proteins in their hepatocytes develop acute vial hepatitis after adoptive transfer of CD8-positive, HBsAg-specific CTL lines and clones (6, 24). Various established HBsAg-specific CTL clones produce TNF-α following HBsAg stimulation (2). Moreover, it was reported that anti-TNF-α Abs (the soluble form of TNFR) markedly blocked the development of hepatitis induced by HBsAg-specific CTLs in HBsAg-Tg mice (22). These results indicated that TNF-α is deeply involved in the progress of liver injury in acute viral hepatitis. Although activated HBsAg-specific CTLs produce TNF-α in fulminant hepatitis, it is considered that TNF-α secreted from only HBsAg-specific CTLs is not enough to cause necroinflammatory liver disease because only 22 CTLs infiltrate in the liver tissue per mm^2 (25). Therefore, TNF-α secreted by non-Ag-specific cells seems to play a critical role in the fulminant hepatitis, but this issue remains to be elucidated.

In this study, we first found that necroinflammatory liver disease did not occur in HBsAg-Tg/TNF-$\alpha^{-/-}$ mice that had received even a large number of HBsAg-specific CTLs. Furthermore, there were no deaths among HBsAg-Tg/TNF-$\alpha^{-/-}$ mice that had received 1.5×10^7 HBsAg-specific CTLs, which caused lethal liver disease in all HBsAg-Tg/TNF-$\alpha^{+/+}$ mice (Fig. 2*B*). Although the peak of severe liver injury was observed within 24–48 h after the CTL injection in this murine hepatitis model, similar injury was not observed in HBsAg-Tg/TNF-$\alpha^{-/-}$ mice at the same time (Fig. 1*B*). When HBsAg-specific CTLs were administered at an extremely high dose into HBsAg-Tg/TNF-$\alpha^{-/-}$ mice, the sALT level slightly increased at 96 h after the CTL injection (Fig. 2*A*). These data suggest that TNF-α secreted by host cells other than Ag-specific CTLs plays a critical role in the acute progression of necroinflammatory liver disease, and it may cause acute hepatitis to develop into lethal liver disease.

In previous studies, it was thought that intrahepatic macrophages mainly produced TNF-α and had the potential to damage hepatocytes in the murine hepatitis model (26). In this model, it was clear that cells of the monocyte/macrophage lineage dominated the inflammatory infiltrate (6). Because the irradiation slightly attenuated the liver injury in this model but did not prevent the massive destruction of most hepatocytes, it can be said that the macrophage lineage plays the major role in this murine fulminant hepatitis (6). However, NK-positive cells (including NKT cells) are also resistant to irradiation (27) and are the second largest mononuclear cell population in the liver after macrophages (Kupffer cells). Therefore, it is possible that the TNF-α secreted by NK-positive cells plays an important role in this model. In contrast, T cells are sensitive to irradiation, and non-Ag-specific T cells in the liver were killed by the irradiation. Thus, the mild decrease in the sALT levels with irradiation as described above can be accounted for by the depletion of the non-Ag-specific T cells in the liver. Taken together, TNF-α secreted by NK-positive cells and non-Ag-specific T cells including CD8-positive cells may play a partially important role in this model.

In vivo, IFN-γ is released by activated HBsAg-specific CTLs when they recognize Ags. Pretreatment with anti-IFN-γ Abs in this murine fulminant hepatitis model completely inhibited the CTL-induced liver injury (6). IFN-γ administration caused marked elevations in the sALT levels in HBsAg-positive Tg mice, whereas it was entirely nontoxic to HBsAg-negative Tg controls (28). In contrast, the Tg and control mice were similarly sensitive to the hepatocytotoxic effects of TNF-α (28). Therefore, we next examined the direct effect of IFN-γ and TNF-α in HBsAg-Tg/TNF-$\alpha^{+/+}$ and HBsAg-Tg/TNF-$\alpha^{-/-}$ mice. IFN-γ administration enhanced the sALT levels in the HBsAg-Tg/TNF-$\alpha^{+/+}$ mice compared with those in the HBsAg-Tg/TNF-$\alpha^{-/-}$ and non-Tg mice (Fig. 5). To confirm the hepatotoxic ability of TNF-α in HBsAg-Tg/TNF-$\alpha^{+/+}$ and HBsAg-Tg/TNF-$\alpha^{-/-}$ mice, we measured the serum ALT level in HBsAg-Tg/TNF-$\alpha^{+/+}$ and HBsAg-Tg/TNF-$\alpha^{-/-}$ mice after the administration of recombinant murine TNF-α. Recombinant murine TNF-α similarly induced liver injury in HBsAg-Tg/TNF-$\alpha^{+/+}$ and HBsAg-Tg/TNF-$\alpha^{-/-}$ mice (data not shown). It is possible that the hepatotoxic response to TNF-α in the HBsAg-Tg/TNF-$\alpha^{+/+}$ mice was similar to that in the HBsAg-Tg/TNF-$\alpha^{-/-}$ mice. IFN-γ secreted by activated CTLs may trigger the enhancement of TNF-α production by non-Ag-specific host cells. The results demonstrated the occurrence of necroinflammatory liver disease in the HBsAg-Tg/TNF-$\alpha^{+/+}$ mice that had received HBsAg-specific CTLs. In the primary culture, the hepatocytes from HBsAg-Tg mice were not destroyed by the addition of high-dose recombinant TNF-α to the culture medium (data not shown). However, it is possible that TNF-α directly exerts its effects to destroy the hepatocytes of HBsAg-Tg mice in this fulminant hepatitis model, because mRNA expression of TNFR1 was up-regulated after the CTL injection. Moreover, the kinetics of sALT levels and the mRNA expression of TNFR1 were quite similar after the CTL injection. These data indicate that TNF-α produced by non-Ag-specific cells may directly destroy the hepatocytes of HBsAg-Tg mice because of CTL-induced enhancement of TNFR1 expression on hepatocytes. However, our data suggests that TNF-α secreted by non-Ag-specific cells plays a critical role in the progression of fulminant hepatitis. In severe viral necroinflammatory liver disease, anti-TNF therapy is thought to be one of the effective treatments.

In summary, we established HBsAg-Tg/TNF-$\alpha^{-/-}$ mice to investigate the role of TNF-α in liver injury caused by CTLs, and demonstrated that TNF-α produced by intrahepatic non-Ag-specific inflammatory cells is critical in the pathogenesis of acute and lethal necroinflammatory liver disease. Anti-TNF therapy may

provide therapeutic benefit to acute viral fulminant hepatitis patients. In contrast, a recent study reported hepatitis B reactivation in a chronic hepatitis B surface Ag carrier after therapy with anti-TNF Ab. Therefore, in severe viral necroinflammatory liver disease, anti-TNF therapy is thought to be an effective treatment. However, anti-TNF therapy should not be administered to patients with persistent HBV infection without careful consideration.

Acknowledgments

We thank Dr. Francis V. Chisari (The Scripps Research Institute) for providing the HBsAg-Tg mice and an HBsAg-specific $CD8^+$ CTL clones (designated 6C2), and Akira Hara for excellent technical assistance. We express our gratitude to John Cole for reading our draft and giving us suggestions on language and style.

Disclosures

The authors have no financial conflict of interest.

References

1. Thimme, R., S. Wieland, C. Steiger, J. Ghrayeb, K. A. Reimann, R. H. Purcell, and F. V. Chisari. 2003. $CD8^+$ T cells mediate viral clearance and disease pathogenesis during acute hepatitis B virus infection. *J. Virol.* 77: 68–76.
2. Ishikawa, T., D. Kono, J. Chung, P. Fowler, A. Theofilopoulos, S. Kakumu, and F. V. Chisari. 1998. Polyclonality and multispecificity of the CTL response to a single viral epitope. *J. Immunol.* 161: 5842–5850.
3. Nakamoto, Y., L. G. Guidotti, V. Pasquetto, R. D. Schreiber, and F. V. Chisari. 1997. Differential target cell sensitivity to CTL-activated death pathways in hepatitis B virus transgenic mice. *J. Immunol.* 158: 5692–5697.
4. Guidotti, L. G., T. Ishikawa, M. V. Hobbs, B. Matzke, R. Schreiber, and F. V. Chisari. 1996. Intracellular inactivation of the hepatitis B virus by cytotoxic T lymphocytes. *Immunity* 4: 25–36.
5. Shresta, S., C. T. Pham, D. A. Thomas, T. A. Graubert, and T. J. Ley. 1998. How do cytotoxic lymphocytes kill their targets? *Curr. Opin. Immunol.* 10: 581–587.
6. Ando, K., T. Moriyama, L. G. Guidotti, S. Wirth, R. D. Schreiber, H. J. Schlicht, S. N. Huang, and F. V. Chisari. 1993. Mechanisms of class I restricted immunopathology: a transgenic mouse model of fulminant hepatitis. *J. Exp. Med.* 178: 1541–1554.
7. Muto, Y., K. T. Nouri-Aria, A. Meager, G. J. Alexander, A. L. Eddleston, and R. Williams. 1988. Enhanced tumour necrosis factor and interleukin-1 in fulminant hepatic failure. *Lancet* 2: 72–74.
8. Zylberberg, H., A. C. Rimaniol, S. Pol, A. Masson, D. De Groote, P. Berthelot, J. F. Bach, C. Brechot, and F. Zavala. 1999. Soluble tumor necrosis factor receptors in chronic hepatitis C: a correlation with histological fibrosis and activity. *J. Hepatol.* 30: 185–191.
9. Vassalli, P. 1992. The pathophysiology of tumor necrosis factors. *Annu. Rev. Immunol.* 10: 411–452.
10. Banchereau, J., F. Briere, C. Caux, J. Davoust, S. Lebecque, Y. J. Liu, B. Pulendran, and K. Palucka. 2000. Immunobiology of dendritic cells. *Annu. Rev. Immunol.* 18: 767–811.
11. Ando, K., K. Hiroishi, T. Kaneko, T. Moriyama, Y. Muto, N. Kayagaki, H. Yagita, K. Okumura, and M. Imawari. 1997. Perforin, Fas/Fas ligand, and TNF-α pathways as specific and bystander killing mechanisms of hepatitis C virus-specific human CTL. *J. Immunol.* 158: 5283–5291.
12. Braun, M. Y., B. Lowin, L. French, H. Acha-Orbea, and J. Tschopp. 1996. Cytotoxic T cells deficient in both functional fas ligand and perforin show residual cytolytic activity yet lose their capacity to induce lethal acute graft-versus-host disease. *J. Exp. Med.* 183: 657–661.
13. Kagi, D., F. Vignaux, B. Ledermann, K. Burki, V. Depraetere, S. Nagata, H. Hengartner, and P. Golstein. 1994. Fas and perforin pathways as major mechanisms of T cell-mediated cytotoxicity. *Science* 265: 528–530.
14. Taniguchi, T., M. Takata, A. Ikeda, E. Momotani, and K. Sekikawa. 1997. Failure of germinal center formation and impairment of response to endotoxin in tumor necrosis factor α-deficient mice. *Lab. Invest.* 77: 647–658.
15. Ohteki, T., R. Okuyama, S. Seki, T. Abo, K. Sugiura, A. Kusumi, T. Ohmori, H. Watanabe, and K. Kumagai. 1992. Age-dependent increase of extrathymic T cells in the liver and their appearance in the periphery of older mice. *J. Immunol.* 149: 1562–1570.
16. Trobonjaca, Z., F. Leithauser, P. Moller, R. Schirmbeck, and J. Reimann. 2001. Activating immunity in the liver, I: liver dendritic cells (but not hepatocytes) are potent activators of IFN-γ release by liver NKT cells. *J. Immunol.* 167: 1413–1422.
17. Meyer, R. A., and M. C. Duffy. 1993. Spontaneous reactivation of chronic hepatitis B infection leading to fulminant hepatic failure: report of two cases and review of the literature. *J. Clin. Gastroenterol.* 17: 231–234.
18. Wright, T. L., and J. Y. Lau. 1993. Clinical aspects of hepatitis B virus infection. *Lancet* 342: 1340–1344.
19. Chisari, F. V. 1995. Hepatitis B virus transgenic mice: insights into the virus and the disease. *Hepatology* 22: 1316–1325.
20. Sugiyama, M., Y. Tanaka, T. Kato, E. Orito, K. Ito, S. K. Acharya, R. G. Gish, A. Kramvis, T. Shimada, N. Izumi, et al. 2006. Influence of hepatitis B virus genotypes on the intra- and extracellular expression of viral DNA and antigens. *Hepatology* 44: 915–924.
21. Ozasa, A., Y. Tanaka, E. Orito, M. Sugiyama, J. H. Kang, S. Hige, T. Kuramitsu, K. Suzuki, E. Tanaka, S. Okada, et al. 2006. Influence of genotypes and precore mutations on fulminant or chronic outcome of acute hepatitis B virus infection. *Hepatology* 44: 326–334.
22. Kondo, T., T. Suda, H. Fukuyama, M. Adachi, and S. Nagata. 1997. Essential roles of the Fas ligand in the development of hepatitis. *Nat. Med.* 3: 409–413.
23. Saunders, B. P., T. Masaki, T. Sawada, S. Halligan, R. K. Phillips, T. Muto, and C. B. Williams. 1995. A peroperative comparison of Western and Oriental colonic anatomy and mesenteric attachments. *Int. J. Colorectal. Dis.* 10: 216–221.
24. Moriyama, T., S. Guilhot, K. Klopchin, B. Moss, C. A. Pinkert, R. D. Palmiter, R. L. Brinster, O. Kanagawa, and F. V. Chisari. 1990. Immunobiology and pathogenesis of hepatocellular injury in hepatitis B virus transgenic mice. *Science* 248: 361–364.
25. Ando, K., L. G. Guidotti, S. Wirth, T. Ishikawa, G. Missale, T. Moriyama, R. D. Schreiber, H. J. Schlicht, S. N. Huang, and F. V. Chisari. 1994. Class I-restricted cytotoxic T lymphocytes are directly cytopathic for their target cells in vivo. *J. Immunol.* 152: 3245–3253.
26. Streetz, K., L. Leifeld, D. Grundmann, J. Ramakers, K. Eckert, U. Spengler, D. Brenner, M. Manns, and C. Trautwein. 2000. Tumor necrosis factor α in the pathogenesis of human and murine fulminant hepatic failure. *Gastroenterology* 119: 446–460.
27. Halder, R. C., S. Seki, A. Weerasinghe, T. Kawamura, H. Watanabe, and T. Abo. 1998. Characterization of NK cells and extrathymic T cells generated in the liver of irradiated mice with a liver shield. *Clin. Exp. Immunol.* 114: 434–447.
28. Gilles, P. N., D. L. Guerrette, R. J. Ulevitch, R. D. Schreiber, and F. V. Chisari. 1992. HBsAg retention sensitizes the hepatocyte to injury by physiological concentrations of interferon-γ. *Hepatology* 16: 655–663.

Chemico-Biological Interactions 182 (2009) 159–164

Contents lists available at ScienceDirect

Chemico-Biological Interactions

journal homepage: www.elsevier.com/locate/chembioint

(−)-Epigallocatechin gallate prevents carbon tetrachloride-induced rat hepatic fibrosis by inhibiting the expression of the PDGFRβ and IGF-1R☆

Yoichi Yasuda[a], Masahito Shimizu[a,*], Hiroyasu Sakai[a], Junpei Iwasa[a], Masaya Kubota[a], Seiji Adachi[a], Yosuke Osawa[a], Hisashi Tsurumi[a], Yukihiko Hara[b], Hisataka Moriwaki[a]

[a] Department of Internal Medicine, Gifu University Graduate School of Medicine, Gifu, Japan
[b] Tea Solutions, Hara Office Inc., Tokyo, Japan

ARTICLE INFO

Article history:
Received 16 June 2009
Received in revised form 13 July 2009
Accepted 22 July 2009
Available online 30 July 2009

Keywords:
EGCG
Liver fibrosis
PDGFRβ
IGF-1R
CCl_4

ABSTRACT

Hepatic fibrosis is a major complication of various chronic liver diseases. Activated hepatic stellate cells (HSCs) play a critical role in the development of liver fibrosis and the axis of platelet-derived growth factor (PDGF)/PDGF receptor (PDGFR), a member of receptor tyrosine kinases (RTKs), is closely associated with the activation of HSC. Insulin-like growth factor (IGF)-1 receptor (IGF-1R), which also belongs to RTKs, interacts with the PDGF/PDGFR axis, thereby cooperatively promoting hepatic fibrosis. We herein examined the effects of (−)-epigallocatechin gallate (EGCG), which inhibits the activation of several types of RTKs, on the development of rat liver fibrosis induced by carbon tetrachloride (CCl_4). Drinking water with 0.1% EGCG significantly decreased the serum levels of both aspartate aminotransferase and alanine aminotransferase raised by CCl_4, thus indicating an improvement of liver injury. In CCl_4-injected rats, EGCG markedly attenuated hepatic fibrosis and decreased the amount of hydroxyproline in the experimental liver. The expression of PDGFRβ and IGF-1R mRNAs in the liver was significantly lowered by the treatment with EGCG. EGCG also decreased the expression of PDGFRβ and α-smooth muscle actin proteins, thus indicating the inhibition of HSC activation. These findings suggest that EGCG can exert, at least in part, an anti-fibrotic effect on the liver by targeting PDGFRβ and IGF-1R. EGCG might therefore be useful in both the prevention and treatment of hepatic fibrosis.

1. Introduction

Hepatic fibrosis is a common response to chronic liver injury from a variety of causes, including infection with hepatic viruses, drug-related, alcohol and metabolic disorders [1]. Progressive fibrosis eventually leads to cirrhosis which is often associated with a high risk of liver failure and hepatocellular carcinoma (HCC) [1,2]. Therefore, the inhibition and prevention of the development of fibrosis might be an effective strategy to improve the prognosis of patients with chronic liver disease. Indeed, recent clinical trials have revealed that treatment with interferon prevents or delays the development of liver cirrhosis and HCC in patients with chronic viral hepatitis [3,4].

The activation of hepatic stellate cells (HSCs) plays a key role in the development of liver fibrosis because activated HSCs are major cellular source of collagen in the injured liver [1]. Following liver injury of any etiology, quiescent HSCs transform to activated cells, which are proliferative and fibrogenic [1]. Several types of growth factors, cytokines, chemokines and their cognate receptors are associated with this transition. Among these factors, autocrine signaling by platelet-derived growth factor (PDGF), which binds to and activates PDGF receptor (PDGFR), is regarded as one of the most potent mitogens and chemotactics for HSCs [5]. The expressions of PDGF and the beta isoform of its receptor (PDGFRβ) have been shown to increase in both experimental rat and human models of liver fibrosis [6,7]. These findings suggest that the activated PDGF/PDGFR signaling pathway may therefore be a candidate therapeutic target for antifibrogenic therapy in liver disease.

Numerous *in vivo* and *in vitro* studies suggest that green tea catechins can exert both cancer therapeutic and cancer preventive

Abbreviations: ALT, alanine aminotransferase; AST, aspartate aminotransferase; α-SMA, α-smooth muscle actin; EGCG, (−)-epigallocatechin gallate; EGFR, epidermal growth factor receptor; ERK, extracellular signal-regulated kinase; HCC, hepatocellular carcinoma; HSC, hepatic stellate cell; IGF-1R, insulin-like growth factor-1 receptor; PDGF, platelet-derived growth factor; PDGFR, PDGF receptor; RTK, receptor tyrosine kinase.

☆ This work was supported in part by Grants-in-Aid from the Ministry of Education, Science, Sports and Culture of Japan (No. 18790457 to M.S. and No. 17015016 to H.M.).

* Corresponding author at: Department of Medicine, Gifu University Graduate School of Medicine, 1-1 Yanagido, Gifu 501-1194, Japan. Tel.: +81 58 230 6313; fax: +81 58 230 6310.
E-mail address: shimim-gif@umin.ac.jp (M. Shimizu).

0009-2797/$ – see front matter © 2009 Elsevier Ireland Ltd. All rights reserved.
doi:10.1016/j.cbi.2009.07.015

properties at various organ sites [8]. One of the anticancer mechanisms of green tea or its constituents is explained by their inhibitory effect on the expression and activation of specific receptor tyrosine kinases (RTKs), such as epidermal growth factor receptor (EGFR), insulin-like growth factor (IGF)-1 receptor (IGF-1R) and PDGFRβ, and related downstream signaling pathways [9–12]. In the present study we investigated the effects of (−)-epigallocatechin gallate (EGCG), the major biologically active component of green tea, on liver fibrosis and on the expression of PDGFRβ using a rat model of carbon tetrachloride (CCl_4)-induced hepatic fibrosis. We also examined whether EGCG alters the expression of IGF-1R in the fibrotic liver because this RTK is closely associated with the PDGF/PDGFR axis and thus plays an important role in liver fibrosis [13].

2. Materials and methods

2.1. Animals and chemicals

Four-week-old male Wistar rats were obtained from Japan SLC, Inc. (Shizuoka, Japan). CCl_4 was purchased from Sigma Chemical Co. (St. Louis, MO). EGCG was provided by the Mitsui Norin Co., Ltd. (Tokyo, Japan).

2.2. Animal protocol

All rats were maintained at Gifu University Life Science Research Center, according to the Institutional Animal Care Guidelines, and were housed in plastic cages with free access to drinking water (tap water supplemented with or without EGCG) and a pelleted basal diet, CRF-1 (Oriental Yeast Co., Ltd., Tokyo, Japan). After 1 week of acclimatization, a total of 26 rats were randomly divided into 4 groups. Groups 1 and 2 (5 rats per group) received an intraperitoneal injection of olive oil (0.5 ml/kg body weight, twice a week) for 8 weeks. Groups 3 and 4 (8 rats per group) received an intraperitoneal injection of CCl_4 (0.5 ml/kg body weight, twice a week) for the same period of time. At the start of the intraperitoneal injections, the rats in Groups 2 and 4 were given tap water containing 0.1% EGCG. The rats in Groups 1 and 3 were given only tap water throughout the experiments. A freshly prepared solution of EGCG in tap water was supplied to the experimental rats three times a week. At the termination of the experiment (13 weeks of age), all rats were sacrificed by CO_2 asphyxiation to determine the development of hepatic fibrosis.

2.3. Histopathological and immunohistochemical examinations

In all experimental groups, 3–4 μm thick sections of 10% buffered formaldehyde-fixed and paraffin-embedded livers were stained with either hematoxylin and eosin (H&E) for histopathology or Azan stain to observe liver fibrosis. Immunohistochemistry of α-smooth muscle actin (α-SMA) was performed using a primary anti-α-SMA antibody (DAKO, Glostrup, Denmark) with paraffin-embedded sections, as previously described [14]. Computer-assisted quantitative analyses of fibrosis development were carried out using the WinROOF image-processing software program (Mitani Corp., Tokyo, Japan) in three low power (×40) fields per specimen, as previously described [14].

2.4. Hepatic hydroxyproline analysis

The hepatic hydroxyproline content (μmol/g wet liver) was quantified colorimetrically in duplicate samples from approximately 200 mg wet-weight of liver tissues, as previously described [15].

2.5. Clinical chemistry

At sacrifice, blood samples were collected from the inferior vena cava and the serum activities of aspartate aminotransferase (AST) and alanine aminotransferase (ALT) were measured using a standard clinical automatic analyzer (type 726, Hitachi, Tokyo, Japan).

2.6. Protein extraction and Western blot analysis

Equivalent amounts of protein lysates (30 μg/lane) from the liver of experimental rats were subjected to a Western blot analysis, as described previously [16]. Anti-PDGFRβ antibody was obtained from Santa Cruz Biotechnology, Inc. (Santa Cruz, CA). Anti-α-smooth muscle actin (α-SMA) antibody was from DAKO. An antibody to GAPDH (Chemicon International, Temecula, CA) served as a loading control.

2.7. RNA extraction and quantitative real-time reverse transcription-PCR analysis

A quantitative real-time reverse transcription-PCR (RT-PCR) analysis was performed, as described previously [17]. Total RNA was isolated from the liver of the experimental rats using the RNAqueous-4PCR kit (Ambion Applied Biosystems, Austin, TX), according to the manufacturer's protocol. The cDNA was synthesized from 0.2 μg of total RNA using SuperScript III First-Strand Synthesis System (Invitrogen, San Diego, CA). The primers used for the amplification of *PDGFRβ*, *IGF-1R* and *GAPDH* specific genes are described previously [18,19]. Real-time PCR was done in a LightCycler (Roche Diagnostics Co., Indianapolis, IN) with SYBR Premix Ex Taq (TaKaRa Bio Inc., Shiga, Japan). The expression level of both the *PDGFRβ* and *IGF-1R* genes was normalized to the *GAPDH* gene expression level. Each experiment was done in triplicate and the average was then calculated.

2.8. Statistical analysis

The data are expressed as the mean ± SD. The statistical significance of the difference in the mean values was evaluated using one-way analysis of variance (ANOVA) and the unpaired *t*-test. Significance was defined as a p value of less than 0.05. All analyses were performed using the StatView ver. 5.0 software (SAS Institute, Cary, NC).

3. Results

3.1. Effects of EGCG on the serum levels of AST and ALT in CCl_4-injected rats

As shown in Fig. 1, the serum AST and ALT levels significantly increased in the CCl_4-injected group (Group 3, $p < 0.01$) in comparison to the control group (Group 1, olive oil-injected group), but they did not increase in the treatment with EGCG alone (Group 2). When compared to the CCl_4-treated group, drinking water with 0.1% EGCG (Group 4) gave lower serum levels of both AST ($p < 0.01$) and ALT ($p < 0.01$), thus indicating suppression of the liver injury (Fig. 1).

3.2. Effects of EGCG on the liver fibrosis in CCl_4-injected rats

Examinations of the Azan-stained sections indicated that treatment with CCl_4 resulted in the development of marked liver fibrosis (Fig. 2C and G). On the other hand, drinking water with 0.1% EGCG significantly prevented the liver fibrosis in comparison to the CCl_4-injected group (Fig. 2D and H). No evidence of fibrosis was observed